12-1-2012

Elemental Contributions from Minor and Major Constituents of Bone on the Separation of Radiostrontium

Ashlee Rae Dailey
University of Nevada, Las Vegas, crable.dailey@gmail.com

ELEMENTAL CONTRIBUTIONS FROM MINOR AND MAJOR CONSTITUENTS OF BONE ON THE SEPARATION OF RADIOSTRONTIUM

By

Ashlee Rae Dailey (Crable)

Bachelor of Arts, German

University of Nevada, Las Vegas

2005

Bachelor of Arts, Chemistry

University of Nevada, Las Vegas

2007

A thesis submitted in partial fulfillment

of the requirements for the

Master of Science in Chemistry

Department of Chemistry

College of Sciences

The Graduate College

University of Nevada, Las Vegas

December 2012

THE GRADUATE COLLEGE

We recommend the thesis prepared under our supervision by

Ashlee Rae Dailey

entitled

Elemental Contributions from Minor and Major Constituents of Bone on the Separation of Radiostrontium

be accepted in partial fulfillment of the requirements for the degree of

Master of Science in Chemistry
Department of Chemistry

Ken Czerwinski, Ph.D., Committee Co-Chair

Ralf Sudowe, Ph.D., Committee Co-Chair

Kathleen Robins, Ph.D., Committee Member

David Hatchett, Ph.D., Committee Member

Ken Moody, Ph.D., Committee Member

Ralph Buechler, Ph.D., Graduate College Representative

Tom Piechota, Ph.D., Interim Vice President for Research &
Dean of the Graduate College

December 2012

ABSTRACT

EFFECTS OF ENVIRONMENTAL MATRIX CONSTITUENTS ON RADIOSTRONTIUM ANALYSIS IN BONE ASH SAMPLES

By

Ashlee R. Crable

Dr. Ralf Sudowe, Examination Committee Chair

Associate Professor of Health Physics and Radiochemistry

University of Nevada, Las Vegas

While many methods exist to separate and analyze radionuclides from a variety of environmental matrices, the performance of all of these methods is often limited by other interfering constituents that are consistently found in most of these samples. The presence of such constituents can significantly reduce the recovery of the radioisotopes of interests and lead to incomplete separations.

Strontium has the same oxidation state and a similar atomic radius as calcium and is therefore readily able to substitute for calcium in lattice sites. This similarity in behavior leads to the preferential accumulation of strontium in newly formed bone. The study of radiostrontium uptake and the analysis of bone samples is therefore of great interest for radiation biology, internal dosimetry, and consequence management. The fact that one of the strontium isotopes of greatest biological importance, ^{90}Sr, is a pure beta-emitter prevents the use of non-destructive assay techniques and necessitates the development of sophisticated separation methods for radiochemical analysis.

It has been previously reported in the literature that the matrix constituents present in bone can significantly affect the strontium recovery from bone samples [1]. Bone (hydroxyapatite) is of particular interest when evaluating the effect of common environmental interferences due to the high concentrations of calcium and phosphate present. The goal of this work is to determine the major and minor constituents present in various samples of bone ash and to determine their influence on method performance and strontium recovery. The work presented exploited the use of a variety of radioanalytical separation and isotope detection techniques. Focusing on the characterization of the bone ash, Scanning Electron Microscopy and X-ray Powder Diffraction techniques were used to determine the morphology, to verify the crystalline pattern, and to analyze for any contaminants within each unique bone ash sample. The information obtained helped to determine the elements of interest for batch experiments, which were conducted in order to determine the individual elemental effects that may play a role on the retention of radiostrontium isotopes onto the SR Resin purchased from Eichrom Technologies Inc. The final set of experiments performed were column studies, which focused on the separation of radiostrontium, recovery yields, and the effect of common environmental contaminants on the separation as a whole. Techniques for the detection of radioactive and stable strontium included Liquid Scintillation Counting, Gamma Spectroscopy, and Inductively Coupled Plasma – Atomic Emissions Spectroscopy.

TABLE OF CONTENTS

LIST OF TABLES

LIST OF FIGURES

CHAPTER 1

1. INTRODUCTION

1.1 Background

A large percentage of nuclear fallout still in existence comes from post 1945 nuclear weapon tests and a small percentage from the accidental release of nuclear materials from the Chernobyl incident and nuclear waste discharge, which combined have led to an alarming concern for the biological consumption of contaminated vegetation and/or animals [1]. The three categories below describe the dietary pathways of radionuclide exposure to man. Category I refers to the pasture-cow-milk-man pathway [2] and is indicative of the initial effects of acute radiation contamination of pasture. Category II is mostly concerned with the use of feed crops and plant products over the course of the first year. Category III is primarily concerned with the long-term transmission of radionuclides, specifically ^{90}Sr and residual ^{137}Cs, through soil and plants [2]. Due to the chemical similarities to calcium, radiostrontium readily incorporates itself into the crystal lattice of bone, particularly marrow [2, 3], most often during the turnover of new cells [4]. The effects on human tissue upon ingestion of irradiated foliage, animals, and/or animal products depends greatly on the chemical properties of the elements, the physiology of the preferred organ(s) as well as size, and on the biological half-life of the radionuclide. Bone marrow is an essential component of the lymphatic system, giving rise to new blood cells and leaving cells vulnerable to the localized high energy beta emissions released by radiostrontium. These could cause serious damage to the blood forming stem cells in bone, and potentially cancer [5].

Strontium-89 is a hazardous radionuclide of immediate concern after a nuclear detonation, mainly attributed to its shorter half-life of 50.57 days. In regards to prolonged effects, ^{90}Sr, one of the most hazardous fission products released into the environment [6], is of greatest concern due to the longer half-life of 28.7 years.

Habitually, radiochemical separations and the analysis of environmental samples require complex methodology owing to potential interferences and require a considerable amount of effort and time, often days, to obtain results [7]. The detection of ^{89}Sr and ^{90}Sr can be challenging due to their primary decay mode of beta particle emissions. Strontium-89 decays not only through emissions of a beta particle but also by a very weak gamma ray, which generally is not substantial enough to provide reliable measurements. Strontium-90, referred to as a pure beta emitter because its only mode of decay is through beta emission, is often more of a challenge to detect due to the in-growth of its daughter product, ^{90}Y, which also decays predominantly through beta emissions, with a very weak gamma ray associated. A limited number of radiation detection instruments are capable of properly detecting broad, and often shifted, spectra of beta particles. Additionally, discrimination among various beta emitting radionuclides simultaneously present is often challenging; therefore a more intricate method is often necessary for detection of both radiostrontium isotopes. Generally radiostrontium must be separated from its daughter product(s) and almost always from other matrix isotopes that may interfere with the analysis. Consequently, understanding the contributions on the separation and/or the detection of radiostrontium of common ions and species found in environmental samples can help in the analysis and determination of radiostrontium levels after a nuclear incident.

1.2 Distribution Ratios

Distribution ratios can be used to determine how well a species is extracted into another phase within solvent extraction systems. This measurement is not usually reported directly in extraction chromatographic systems, but rather indirectly through the D_w, weight distribution ratio, value [8]. The following equation can be used to determine the value of D_w:

$$D_W = \frac{A_0 - A_S}{A_S} \bullet \frac{mL}{g} \quad (1)$$

Where:

$A_0 - A_S$ = sorbed activity of a given metal ion on a known weight of resin, g

A_S = the activity in a known volume, mL, of solution

D_w can then be used to determine the k', the number of free column volumes to peak maximum value for a given metal ion by dividing the D_V conversion factor of 2.19 for SR resin. This originates from the calculation of the volume distribution ratio, D_V (Equation 2) [8]:

$$D_V = D_W - \frac{d_{extr}}{0.4} \tag{2}$$

Where:

d_{extr} is the density of the extractant

0.4 is the extractant loading in grams of extractant per gram of resin

A larger k' value for a given species indicates a higher affinity to the resin. Resins from Eichrom Technologies Inc. often contain an organic extractant, such as (4,4'(5')-di-t-butylcyclohexano 18-crown-6 (crown ether) in 1-octanol) for SR resin, loaded onto an inert chromatographic support, making up the stationary phase and the "matrix" solution that flows through the column, interacts and passes through the resin beads is known as the aqueous, or mobile phase.

1.3 Eichrom Resins

Eichrom Technologies, Inc. offer commercially available resins that can be used for the extraction chromatographic separations of a variety of samples containing radioisotopes. The resin beads used typically range in size from 50 – 150 μm in diameter, even though both smaller and larger particles have been studied for special applications. SR resin was used in order to assure the complete separation of strontium and/or lead from various sample matrices. Its stationary phase consists of a dicyclohexano 18-crown-6 derivative dissolved in an aliphatic alcohol. The structure, which is ion selective for both charge and size, is shown in Figure 1.

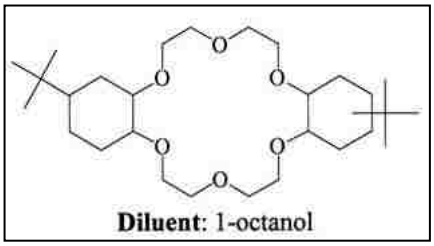

Figure 1 SR Resin. Horwitz, et al.

Acid dependency curves can be helpful tools when developing a separation schematic for a given matrix of interest. Figure 2 shows the nitric acid dependency of k' values for several elements using SR resin. Calcium, being a major component of most environmental samples can often interfere with the separation of radiostrontium, since the atomic radii of both divalent ions are similar. SR resin is more easily separated in higher concentrations of nitric acid; therefore, these studies were conducted in a 4 M nitric acid matrix.

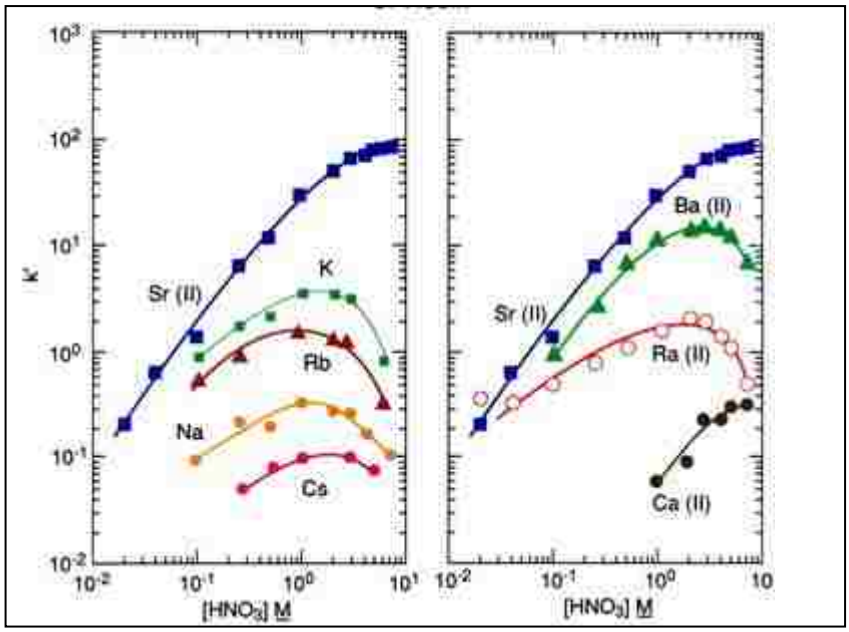

Figure 2 Dependencies for the uptake of selected metal ions by SR Resin. Temperature 23 - 25 °C. Horwitz, et al.

1.4 Batch Distribution Studies

Batch studies provide the ability to identify, isolate, and determine the influences of major and minor constituents present in various environmental matrices of bone on the adsorption of isotopes to extraction chromatographic SR resin. This method is most useful in determining the

relative strength of retention for individual ions onto the resin through determination of the k' trends.

Bone ash consists primarily of calcium and phosphates, however, there are many other contaminants that may exist within bone in small quantities. These quantities may be large enough to affect the uptake of strontium onto the SR resin. In order to observe the contributions of these elements individually, batch experiments need to be performed. Column studies can help in assessing both minor and major matrix constituents under dynamic conditions by means of common laboratory separation procedures.

The affinity of these species to the resin is what determines how well the separation or extraction procedure occurs. As stated previously, this attraction is typically expressed as a k' value or a distribution ratio. In order to determine the effects that an individual ion may have on the separation procedure, k' values for each matrix of interest need to be determined and compared. In order to determine the k' values, an aqueous solution must be allowed to interact and reach a point of equilibrium with a known mass of resin for a suitable amount of time.

1.5 Column Separation Studies

An efficient way of separating elements(s) from a complex matrix based on the chemical properties involves column chromatography. Plastic or glass columns can be loaded with a desired material, such as resin, in order to separate specific ions from their current solution matrix. The material contained in the columns has a preferential attraction towards a specific ion or molecule based on size and/or charge and porosity. Theoretical plates can play a role in the efficiency of the final separation yield. Once the solution is loaded onto the column, the ions of interest adsorb onto the resin and the remaining species elute. The eluted fraction can be collected, and by changing the solution matrices, the adsorbed radionuclides can then be later removed and collected as a separate fraction. Current methods of extraction chromatography involve several aliquots, or fractions, collected and analyzed after each separation. The resin

wetting fraction is often used as an analytical baseline for the experimental set-up since the analyte(s) of interest is(are) not yet introduced. The load and rinse fractions collected consist of the ions that are not adsorbed on the resin once the analyte (s) is added to the column. The final strip fraction represents the species that are bound to the resins, or the analyte (s) separated. The analysis of each fraction can be exploited for the recovery yield calculation, and determination of the desired analyte (s) is identified by comparison to a known standard.

1.6 Radiochemical Separation Techniques

Solvent extraction, co-precipitation, ion exchange, and extraction chromatography are common radioanalytical separation techniques currently used to isolate ions or elements of interest. When separating radiostrontium, solvent extraction and precipitation methods are most commonly used. Solvent extraction, often referred to as liquid-liquid extraction, is a process by which a solute is selectively removed from a liquid mixture containing a solvent. Solutes exhibit different solubilities when in various solvents, for that reason, the extracting solvent(s) and ligand(s) are chosen based on the experimental requirements of the solute. Solute molecules will migrate to the volume portion with either a higher or lower solute concentration in order to reach a point of equilibrium based on the principles of osmosis. It is common in liquid-liquid extraction for layers to form and the solute of interest to be found preferentially in one of the immiscible layers. Often multiple extractions are required, making this method labor intensive. The mixed wastes that are generated are difficult and expensive to dispose of, and toxic solvents are often required; therefore, many laboratories have avoided the use of this separation method for current separation schemes [9].

Co-precipitation combines a selected ion too dilute to precipitate out on its own with a secondary carrier ion of adequate volume and concentration in order to exceed the solubility limit, thus producing a supersaturated solution or compound. To precipitate specific radionuclides out of solution a stable isotope of the same element is used as a carrier to guide in the transition of

crystallization. The carrier permits a better probability of recovery and of precipitation. Other radionuclides that do not have a stable counterpart use elements of the same family, or group, as a substitute because they exhibit similar chemical properties. The precipitate is most likely collected using filtration or centrifugation procedures. Co-precipitation of radiostrontium can be tedious when repetition of steps must be performed in order to obtain sufficient recoveries [10]. Ion exchange involves a chemical reaction between two substances, typically in different physical states, where one or more ionic components are replaced. Insoluble materials bearing either negative or positive surface charges remove various ions, or molecules with a positive or negative charge, by attraction from coulombic force.

Methods involving the use of ion-exchange resin(s) typically require careful control of the pH, which can be difficult for the separation of environmental samples involving calcium, where reasonable separations are achieved only within a narrow pH window [9]. Extraction chromatography utilizing an insoluble resin bead incorporating into an organic material that can selectively bind ions based on their charge, complex stability, and/or size can be used to separate radionuclides of interest; however, the resins can also have a tendency to bleed out when activity levels of radionuclides are high enough or when higher concentrations of acid are left on the columns over night. In current radioanalytical separation techniques, ions often compete against one another for active sites on materials, or resins, thus reducing the efficiency and recovery yield of radiochemical separations. The introduction of crown ether resin has made advancements in the separation efficiencies of radiostrontium in various matrices; however, yields can still be relatively unsatisfactory when higher concentrations of barium and/or calcium are present [9].

For the purpose of analytical measurements in support of emergency response and for the optimization of current forensic analysis techniques, the effect of interferences on separation methods needs to be investigated.

1.7 Extraction Chromatography

Extraction chromatography is a radioanalytical technique that is commonly used to separate isotopes of interest by combining the selectivity of liquid-liquid extraction with the operational ease of column chromatography [8, 11]. EXC (extraction chromatography) systems consist of an inert support, such as porous silica or organic polymer, a stationary phase, single compounds or mixtures of liquid extractants often form this layer, and a mobile phase, usually consisting of acidic solutions such as nitric acid, shown in Figure 3

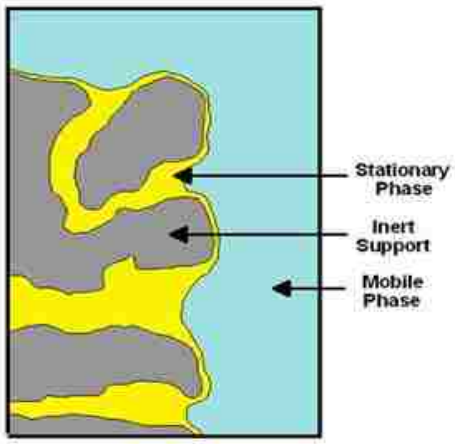

Figure 3 Surface of a porous Eichrom resin bead. Horwitz, et al.

The mobile phase usually varies in its concentrations of nitric or hydrochloric acid in order to aid in the adsorption or extraction of radionuclides from the column. However, complexants like hydrofluoric acid may also be used to enhance the removal of strongly bound metal ions. The rate at which the solutions flow through the resin columns can drastically affect the recovery of the desired species.

The chemical system, particle size and the support porosity, velocity of the extractant loading and mobile phases, and the ambient temperature are all extremely important contributors for the efficiency of the column(s) [8]. Each column contains "theoretical plates" for the length of the column, which can be visualized as a series of bands when ions in solution flow through the columns and interact with resins. The band spreading must be small in order to avoid early

breakthrough of the solution of interest and cross-contamination of samples, as well as obtaining an efficient separation [8].

1.8 Literature Background

Following the nuclear weapons testing during the post WWII era and the awareness of potential health effects from exposure to radionuclides by biological means, an enormous effort to secure radioactive materials from the environment has been put forth. Radionuclides, produced as a result of a self-sustained chain reaction of nuclear fission, vary in energy, activity, mode of decay, as well as the rate of decay. These isotopes are often enriched through food chains and can be ingested, potentially leading to hazardous health conditions or even death depending on the degree of exposure. Of the nuclides produced, actinides are vast and considered to be the most toxic radionuclides in the environment [10], other non-alpha emitting radionuclides, such as ^{90}Sr, are also a high emergency priority due to their hazardous nature [6]. As a preventative measure, in the case of a nuclear emergency, the need to separate as well as isolate and store radioisotopes away from the public has been designated as a priority [12].

Over the past few decades, analytical methods have been probed and further refined in preparation for the separation of radionuclides from complex matrices. Traditional methods are often difficult and time consuming [12] and not capable of providing the desired information rapidly enough in the event of a nuclear incident [7]. Repeated pretreatment and pre-concentration of environmental samples from complex matrices are often necessary and due to the spectra interferences of fission products and their daughters, the species that make up the sample(s) may not be known adequately. Therefore, an early separation step, or several, may be essential in order to determine the most optimal course of sample analysis. More modern methods often employ non-destructive sampling techniques in order to better understand the isotopic elements that are present in the sample matrix prior to sample digestion and reduce sample processing time with the ability to better assess the treatments required. These techniques often include at least

Gamma-ray Spectroscopy or Scanning Electron Microscopy, but can also contain variations of X-ray diffraction, based on the available quantities of sample. Early separation steps have incorporated the use of ion exchange columns to separate out specific elemental molecules, but more current techniques employ the use of resin(s) from Eichrom Technologies Inc., and the exploitation of stacking the column cartridges. This has decreased the forensic analysis time by hours with the assistance of vacuum assisted extraction chromatography [13]. Stacked columns for the analysis of environmental samples often include TRU, TEVA, or UTEVA, and SR, but can be rearranged to include any of the resins available for purchase.

Samples are typically unique and the physical state of sample contaminants can vary tremendously. Solid samples may also contain liquid, creating a slurry, while other samples may contain gaseous isotopes, or radionuclides may eventually decay into gaseous daughter products. Therefore, the process of sample collection is very important and should consider the capture and containment of gaseous products for complete sample analysis and for the ability to select and employ sample processing techniques specific to the sample. For most samples, gases are collected and the remaining material is dry ashed within a muffle furnace for later dissolution. Several repetitions of evaporation followed by dilution may be used to convert the sample to a particular acid medium or to completely remove interfering organic materials and other potential interferents. Complete digestion of the sample into the liquid form is generally carried out by dilution of acid, leaching, fusion techniques, and/or microwave digestion. A carrier and/or sometimes a radiotracer may be incorporated into the sample prior to treatment to prevent the loss of the radionuclides as well as determine the recovery yield of the related isotopes gravimetrically or through radiation detection systems.

Careful monitoring of pH is often a significant consideration when using more traditional methods [12]. Both traditional and modern radioanalytical separation techniques alike have been used to isolate radioisotopes from interfering matrix species. These include ion-exchange, solvent extraction, or liquid-liquid extraction, co-precipitation, and extraction chromatography. Any of

these separations can involve complex chemistry in order to remove specific species from a multifaceted matrix. This can be particularly difficult when the quantity within the sample is minimal, or the solubility constant of the ion(s) is well below the threshold needed to form a quantifiable precipitate. For this reason a carrier or precipitate, preferably of the same element or of similar chemical behavior, would be added to co-precipitate the desired species out of solution. Precipitation can also be useful when separating chemicals from a complex matrix; for example, precipitation of $SrSO_4$ in order to isolate strontium from surrounding barium molecules [14].

Early determination of ^{89}Sr is of great importance during the first week of, and well over a month after a nuclear event due to the shorter physical half-life (50.5 days) [7], and the ability of strontium to readily accumulate in bone [2]. Typically, $^{89/90}Sr$ is isolated from a sample matrix and analyzed by a gas proportional counting system, at which point the isotopes can be separated and counted after the daughter ^{90}Y has grown in, or the entire sample can be recounted and the activity of each isotope is calculated based on their half-lives. A minimum of a five day decay time is highly suggested for ^{89}Sr and at least nine days for the detection of ^{90}Sr, although, Čerenkov counting prior to the decay of radiostrontium can be implemented to facilitate early detection of the isotopes and reduce the analysis time [7]. Prior to alpha spectroscopic analysis, actinides of interest must also be isolated from elemental contributors present in the sample, and other α-emitting radionuclides due to overlapping energies. Preparation of samples for alpha spectroscopy for high recovery yield and energy resolution using electrodeposition or microprecipitation has advanced greatly over the past few decades but can be tedious [15].

Optimization of traditional techniques has contributed to progression in methods for the nuclear forensic analysis as well as emergency preparedness. Elemental effects commonly found within environmental samples, have been shown to contribute to the separation schematics of radionuclides; however, the degree to which these constituents affect the separations is not well known. Important actinides, such as plutonium, uranium, americium, and thorium, as well as some beta emitters, radiostrontium and cesium, have been successfully separated and analyzed

from complex soil matrices, providing ^{90}Sr recoveries well within the recommended range set by the National Physics Laboratory [16]. Additionally, this has greatly improved the common environmental sampling methods. Another material of interest is bone. The affinity of radiostrontium and actinides to the crystal lattice of this organ is of great health concern;. Therefore, procedures have been proposed to detect and identify the levels of radionuclides present in bone and tissues. Direct radiobioassay has been applied to the remains of animals and humans through analysis of bone and bone ash, yielding recovery values of ^{90}Sr greater than 73 ± 2% [17, 18]. Indirect determination of environmental radiostrontium contamination can be verified through studies of milk, a readily available source for the human consumption of strontium. Extensive research has been performed to establish and monitor the radiostrontium activity levels in milk ÷[12, 24]. Although, the effects of calcium on the separation of strontium have been investigated, the elemental effects and contributions of metal ions commonly found in most environmental samples, including bone and bone ash, using extraction chromatography have not been fully probed. Such findings would lead to a better understanding of the direct effects associated with low metal contamination concentrations using modern separation techniques, and would aid in the ability for scientists to develop more optimal forensic methods based on the properties of the sample.

CHAPTER 2

2 MATERIALS AND METHODS

2.1 Batch Distribution Studies

The batch distribution studies enabled the identification and isolation of specific metal ion contributions towards the sorption of radioisotopes onto SR resin. The interaction of ions with the element of interest and resins provided the necessary information for the calculations of k' values and the trends associated, thus giving insight to the behavior of the ions. Loose resins were allowed to equilibrate with a known activity of ^{85}Sr as well as an element, or ion, of interest. Elements and compounds considered included calcium, phosphate, potassium, magnesium, aluminum, sodium, and zirconium. Varied concentrations of each element were analyzed in replicates of five for each concentration observed. Nitrates were already present in the strontium standard, therefore elemental solutions were not mixed with reagents containing large amounts of nitrates, so as not to alter the overall concentration of nitrate ions present in each sample. A consistent aliquot of the supernatant was collected from each sample individually and counted on the gamma spectrometer. For each concentration analyzed, the average of the five samples was taken and the trends were observed.

2.1.1 Methodology

When in the presence of free ions, SR resin can attract and bind cations while anions and neutral species flow past the resins and remain in solution. If the mass of the resin is known and the volume and concentration of acid are also known, then the resin capacity factor, k', can be determined. Collective k' values for a varied set of parameters can reveal contributions, or lack thereof, for specific elemental reactions. A large pool of samples is necessary for confidence in the observed scientific effects and for good statistics.

2.1.2 Time and Mass Study

Kinetic and mass studies were investigated on a small-scale in order to ensure mass independence of the SR resin from Eichrom Technologies and to determine the ideal conditions for the batch experiments. Five trials were analyzed for each mass observed with the mixing time held constant (and vice versa). For each run, five empty plastic microcentrifuge vials were weighed and tared, then loaded with a desired amount of SR resin. Masses observed included 0.50 mg and 0.75 mg. Mixing times observed included 1 hour, 6 hours, and 24 hours.

2.1.3 Elemental Solution Preparation

Ions of interest for this experiment included potassium (I), calcium (II), magnesium (II), aluminum (III), zirconium (IV), and phosphate. Samples were dissolved in 4 M nitric acid and calculations for the amount of salt needed were based on the desired concentration of the ion or compound of interest in the final solution. Salts were carefully selected to optimize the solubility range of the solution and also to ensure nitrates present in solution remained constant in concentration. Sodium was not observed in this study since an adequate salt was not established.

Potassium phosphate monobasic, KH_2PO_4, purchased from Fisher was used to observe the effects that potassium (I) and phosphate have on the adsorption of ^{85}Sr to the SR resin. The solubility of potassium phosphate reaches a maximum at about 95 grams of KH_2PO_4 per 100 grams of water. Utilizing potassium phosphate's molecular weight, 136.0836 g mol^{-1}, for potassium phosphate, the calculations to make concentrations of 0.1, 0.3, 0.5, 0.7, 1.0, 2.0, 3.0, and 3.5 M [K^+] or [PO_4^{3-}] were performed. The desired amount of the KH_2PO_4 salt was added to a clean 50 mL volumetric flask and 4 M nitric acid was added (i.e. 0.6816g of KH_2PO_4 for 0.1 M [K^+]). The solution was swirled and heated if needed until all of the potassium phosphate crystals were dissolved. Then the solution was diluted to the 50 mL mark indicated on the flask. Each solution was transferred to a clean, labeled Nalgene bottle and stored for later use.

Potassium Bromide, KBr, purchased from Sigma-Aldrich was used to observe the effects potassium (I) without the presence of phosphate. The maximum solubility for potassium bromide

is reached at about 67 grams of KBr per 100 grams of water. Calculations to make concentrations of 0.1, 0.2, 0.3, 0.4, 0.5, 1.0, 2.0, 3.0, 4.0, and 5.3 M [K^+] were performed, taking into account molecular weight, 119.01 g mol^{-1}. The desired amount of KBr salt was weighed and then added to a clean 50 mL volumetric flask and then 4 M nitric acid was added (i.e. 0.5904g of potassium bromide for a desired 0.1 M [K^+] solution). The solution was swirled until all salt crystals were dissolved, and then diluted up to the 50 mL mark indicated on the volumetric glass. Each solution was transferred to a clean, labeled Nalgene bottle and stored for later use.

Calcium bromide anhydrous, $CaBr_2$, purchased from Alfa Aesar was used to observe the effects of calcium (II) on the sorption of ^{85}Sr to SR resin. A maximum solubility of calcium bromide is reached at about 135 grams of $CaBr_2$ per 100 grams of water. Calculations to make concentrations of 0.1, 0.2, 0.3, 0.4, 0.5, 1.0, and 2.5 M [Ca^{2+}] were performed, taking the molecular weight, 199.9 g mol^{-1}, of calcium bromide into account. The calculated mass of $CaBr_2$ needed was weighed and added to a clean 50 mL volumetric flask and then diluted with 4 M nitric acid (i.e. 1.000g of calcium bromide for a solution of 0.1 M [Ca^{2+}]). Once all of the calcium bromide salt crystals were dissolved, 4 M nitric was added until 50 mL of solution reached the mark on the volumetric flask. Each solution was transferred to a clean, labeled Nalgene bottle and stored for later use.

Magnesium bromide hexahydrate, $MgBr_2 \bullet 6H_2O$, purchased from Acros Organics was used to observe the effects of magnesium (II). The solubility of magnesium bromide can be as high as 103 grams per 100 grams of water. The calculations for the following concentrations, 0.1, 0.3, 0.5, 1.0, and 4.0 M [Mg^{2+}], were performed taking into account the molecular weight, 292.204 g mol^{-1}, of magnesium bromide (i.e. 1.474 g of $MgBr_2$ for a desired concentration of 0.1 M [Mg^{2+}]). The designated amount of magnesium bromide salt needed was weighed and added to a 50 mL volumetric flask and diluted with 4 M nitric acid. Due to the hydroscopic nature of magnesium bromide, preparing solutions of higher [Mg^{2+}] concentrations was problematic and many of the solutions were heated to assist with the dissolution of the salt. Once the solutions were diluted to

the 50 mL mark in the volumetric flasks, the solutions were then transferred to new, labeled Nalgene bottles and stored for later use.

Aluminum chloride anhydrous, $AlCl_3$, purchased from Alfa Aesar was used to observe the effects of aluminum (III). The solubility of aluminum reaches a maximum at about 46 grams of aluminum chloride per 100 grams of water. The calculations for concentrations of 0.1, 0.3, 0.5, 1.0, 1.5, and 3.0 M [Al^{3+}] were performed utilizing the molecular weight, 133.34 g mol^{-1} of $AlCl_3$ (i.e. 0.679 g for a concentration of 0.1 M [Al^{3+}]). The required salt mass was weighed and transferred to a 50 mL volumetric flask and then diluted with 4 M nitric acid. Once the salt crystals were completely dissolved an additional 4 M nitric acid was added to the volumetric flask 50 mL mark. The solutions were then transferred to new, labeled Nalgene bottles for later use. When making these solutions, it was extremely important that all steps of the reaction be carried out using glass; any plastic (i.e. disposable pipettes) was melted immediately upon exposure to aluminum chloride and nitric acid. Adding the aluminum chloride to the nitric acid contained the extreme reactions that occurred when making these solutions.

Zirconium (IV) Sulfate tetrahydrate, $Zr(SO_4)_2 \cdot 4H_2O$, purchased from Alfa Aesar was used to observe the effects of Zirconium (IV). A maximum solubility of zirconium sulfate can be reached at roughly 52 grams of $Zr(SO_4)_2$ per 100 grams of water. The calculations for the following concentrations, 0.1, 0.3, 0.5, and 1.0 M [Zr^{4+}], were performed taking into account the molecular weight, 355.41 g mol^{-1}, of zirconium sulfate (i.e. 1.779 g of $Zr(SO_4)_2$ for a desired concentration of 0.1 M [Zr^{4+}]. The necessary amount of salt needed for each concentration was weighed out and added to a 50 mL volumetric flask and diluted with 4 M nitric acid. After all of the zirconium sulfate crystals were dissolved, with the help of a hot plate for most samples, additional aliquots of 4 M nitric acid was added in order to reach the 50 mL mark on the volumetric flask. Each solution was then transferred to a new, labeled Nalgene bottle for later use.

2.1.4 Mixing

Samples were mixed using a Thermo Scientific Labquake shaker with a fixed speed. Up to 40 samples were laid on their sides and inverted for a sufficient duration of time, one hour, so that all of the contents in the vials were allowed to thoroughly mix and all reactions would reach a point of equilibrium. All samples, 0.5 mg of SR resin allowed to mix with 1.3 mL of sample solution, were mixed for one hour after the desired ion solution and strontium spike were added.

Figure 4 Labquake Shaker

2.1.5 Filtering

PTFE Whatman syringe filters with a pore size of 0.45 µm were purchased from VWR. The filters were attached, screwed onto Luer-Lok syringes and used to separate the supernatant from the resin and into new, labeled microcentrifuge vials.

Figure 5 Filter and Syringe

2.1.6 Sample Preparation for Analysis

An aliquot of 0.9 mL of the filtered supernatant was transferred to an empty gamma spectrometer vial and diluted to 1 mL with 4 M nitric acid. Each sample was counted on an HPGe detector for three hours.

2.2 Non-destructive Sample Analysis

Several methods of non-destructive sample analysis can be used in order to characterize a solid material prior to sample dissolution and chemical analysis. Characterization of solid matrix materials prior to chemical analysis can serve as a valuable aid when determining which types of chemical analysis should be performed on a sample, particularly unknown samples. From solid matrix characterization techniques we can often gather the major and minor isotopes present, matrix contents, as well as a possible source of origination for the material. Using non-destructive sample techniques can be preferential to prevent loss of valuable sample information which might otherwise be destroyed during homogenization processes. Both SEM and XRD were used prior to sample analysis.

2.2.1 X-ray Powder Diffraction

By using XRD (X-ray Powder Diffraction) to observe the crystallization patterns of the hydroxyapatite, one can determine how much of the sample is bone, and the percentage of distinguishable parts not consisting of bone. Samples were crushed in a mortar and pestle using a small amount of ethyl alcohol. Once evenly pulverized, the samples were smeared onto specialized sample holders using ethyl alcohol. The samples were loaded and run one at a time. EVA and TOPAS software systems were used to determine the matrix components of each sample.

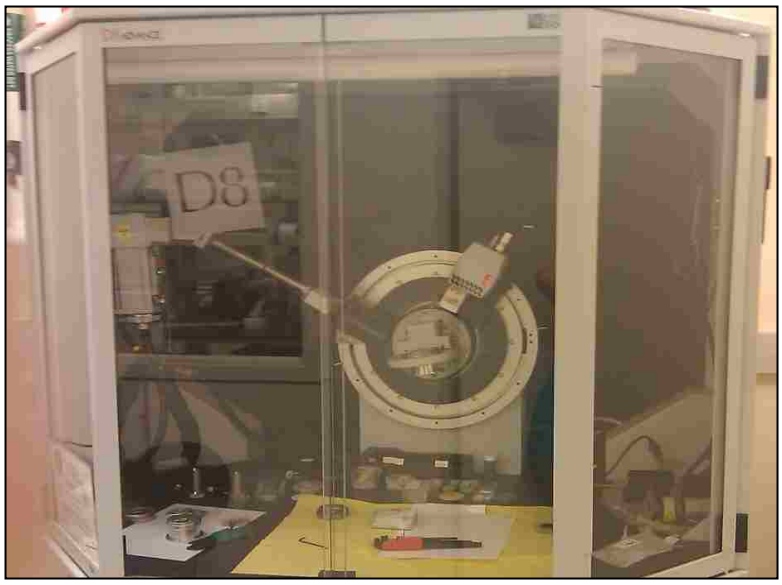

Figure 6 X-ray Powder Diffraction

2.2.2 Scanning Electron Microscopy

SEM (Scanning Electron Microscopy) makes use of electrons, which have shorter wavelengths than visible light thus permitting higher image resolution. Incident electrons that collide with electrons of the sample produce secondary electrons.

Figure 7 Scanning Electron Microscopy with EDS capabilities

If the incident electron interacts with a nucleus from the sample then backscattered electrons result and aid in the determination of differences in density within samples, thus providing an image of the material. A unique feature to Scanning Electron Microscopy is EDS (energy

dispersive x-ray spectroscopy), which provides both qualitative and quantitative elemental analysis of samples. Using this technique bone contaminants were observed. Samples were prepared using the same procedure applied to the XRD samples (see Figures 8 and 9); however, a Cressington Sputter Coater was used to plate SEM samples with an ultrathin layer of electrically-conducting gold (see Figure 10). The coating was implemented in order to prevent the accumulation of static electric charge during irradiation, or flawed images.

Figure 8 Mortar and Pestle

Figure 9 Sample Holder

Figure 10 Gold Plater

2.3 Destructive Sample Analysis

Data can be collected from chemical separations using common spectroscopic techniques such as ICP (inductively coupled plasma) - mass spectrometry or - atomic emission spectroscopy, liquid scintillation counting, or gamma spectrometry. Samples would need to be dissolved and often diluted in an acidic matrix such as nitric acid. Microwave digestion, fusion, and leaching are all common dissolution methods used for soil and ashed materials. Sample dissolution followed by chemical separations were performed and analyzed using various spectroscopic techniques. Batch experiments were only performed using the isotope ^{85}Sr and were therefore able to be counted using a gamma spectrometer. The ion solutions employed were analyzed using ICP-AES.

2.3.1 Microwave Digestion System

A microwave digestion system purchased from Milestone Laboratory was used to dissolve bone ash samples for this project. The Environmental Protection Agency provides approved microwave assisted acid digestion protocols for various sample types. A modified version of EPA Method 3052, a method for digestion of ashes and soils of siliceous and organically based matrices, was used for the dissolution of bone ash samples [19].

2.3.1.1 Apparatus

A closed vessel microwave digestion system, ETHOS EZ, was purchased from Milestone Incorporated. This system has been shown to be both rugged as well as corrosion resistant due to its multi-layer PTFE plasma coating and external user controlled electronics. Specially designed cooling also allows for shorter run times. Pressure can be set to reach 100 bar and temperatures up to 300˚ C in 10 vessels at a time.

Figure 11 Microwave Digestion System

2.3.1.2 System Specifications and Parameters

Calculations were performed for all ions of interest. Vessels were weighed and then tared. The desired amount of bone ash, not to exceed 1.2 g, was then added to the vessel, and the exact weight was recorded. 9 mL of 7.5 M nitric acid were added to the vessel and the final weight including the vessel was recorded. The lids were then placed atop the vessels and inserted into their designated place in the digestion chamber. The pressure was set to 20 bar, the power was set at 1000 W, and the temperature was set to reach 180 ˚C after 5.5 minutes and then remain at 180 ˚C for a 9.5 minutes. The digestion system was programmed to rotate while the vessels were gradually cooled for a 10-minute cycle. Once cooled, the vessel lids were carefully removed and the vessel was weighed. Both the initial mass acquired prior to dissolution and the final mass recorded after digestion were used to ensure sample merit by verifying that no more than 1 % of the solution was lost. The elected samples were then added to a 50 mL volumetric flask and diluted to the mark with the necessary quantities of water and/or nitric acid to obtain a final concentration of 4 M nitric acid. An additional 10 mL of concentrated HNO_3 was added to each

vessel, and a cleaning digestion was performed at a set pressure of 20 bar, power at 500 W, and temperature of 160 ˚C. The temperature remained at 160 ˚C for 10 minutes, and then the vessel was cooled for 10 minutes longer before discarding the contents. A laser pointer was used to observe remaining particulates. No reflections were observed.

2.4 Column Chromatography

Extraction chromatography combines IEC, ion exchange chromatography, with that of solvent extraction in order to increase both selectivity and reduce the volume of waste. By utilization of a pressurized vacuum box, larger pools of samples can be separated and processed and at a much faster rate. Using a vacuum box allows solutions to travel through resin columns at faster flow rates than imposed by gravity. Therefore, separations should be performed at pressure settings that are fixed and closer to ambient pressure setting may be necessary for different sample types.

2.4.1.1 Apparatus

The vacuum boxes, constructed by Rich Gostic Ph.D., used for the column studies could be used to run five to fifteen samples concurrently. Each box contained a fitted lid that was detachable for operational ease, grooves that were intended to fit pre-packed resin cartridges from Eichrom Technologies Inc. tightly, an inner tray designed to fit 50 mL centrifuge tubes for fraction collections, and a clear facing to allow experimental observations. The airtight box was then connected to a vacuum pump as well as a DVR, digital vacuum regulator, in order to control the set parameters for each run, allowing more even solution flow rates. An emergency relief valve was present in order to bring vacuum pressures back to ambient in order to access materials if the need should occur. Julie Gostic Ph.D. using a variety of isotopes, which included radiostrontium, calibrated these boxes at various pressure settings

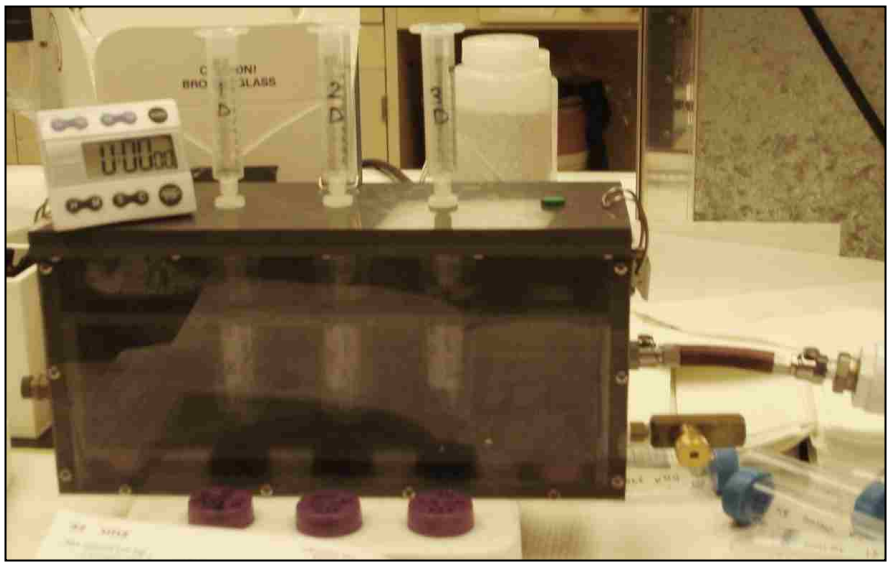

Figure 12 Small pressurized vacuum box

Figure 13 Large pressurized vacuum box

2.4.1.2 System Specifications and Parameters

Separations of ^{90}Sr in nitric acid media were performed and pressure settings close to ambient pressure, 650, 675, and 690 torr, were studied in order to determine optimal experimental conditions. The data observed from the separations ran using the fixed 675 torr pressure setting was saved and used as the standard for future runs. Lids were removed from empty, pre-labeled

50 mL centrifuge tube vials and the vials were set into the inner tray of the vacuum box. The lid was reattached and SR resin columns were inserted into their designated positions in the lid. Syringe tubes (10 mL) with the pump stick removed were then attached atop the resin cartridges. For separations that contained only ^{90}Sr, 5 mL of 4 M HNO_3 was transferred to the syringes and a 6 mL aliquot of 4 M HNO_3 was used instead for separations that also included an ^{85}Sr tracer. The DVR was set to 675 torr and the vacuum was turned on. A timer was used to record the total amount of time required for the entire volume of solution to pass through the columns, yielding the flow rate for each sample. After all of the solution had drained through, the vacuum was turned off and the lid was removed. Once the pressure returned to ambient, the tubes were collected and capped. These samples compose the resin wetting fraction, since the solution was used to wet the resin and activate the sites that were used to attract specific ions of interest. New, empty, pre-labeled 50 mL centrifuge tubes were then placed inside the box and the lid was sealed. For earlier separations including only ^{90}Sr, 2.5 mL of ^{90}Sr in 4 M nitric acid as well as 2.5 mL of a desired concentration of dissolved Bone Ash in 4 M nitric acid were added to the syringes. For separations that also included an ^{85}Sr tracer, 2.5 mL of ^{90}Sr in 4 M nitric acid, 2.5 mL of a desired concentration of dissolved Bone Ash in 4 M nitric acid, and 1 mL of ^{85}Sr in 4 M nitric acid were added to the syringes. The DVR was set to 675 torr and the vacuum was turned on. Once the solutions drained through the column and into the vials, the load fractions were collected, capped, and stored for later counting. The same steps were repeated, rinsing the columns with 3 M nitric acid, 5 mL aliquots were used for separations involving only Sr-90 and 6 mL aliquots for separations, which included an ^{85}Sr tracer. Finally either 5 mL or 6 mL of water was added to the syringe reservoirs. Ideally, all of the radiostrontium added during the load phase was eluted, or stripped at this point. The load, rinse, and strip fractions were analyzed on the LSC and ICP-AES. Samples containing an ^{85}Sr tracer were also counted on the gamma spectrometer. The fractions obtained from the resin wetting phase were analyzed and used as blanks to determine the recovery yield of radiostrontium.

Load concentrations of 8 M nitric acid and 2 M HNO_3 – 0.5 M $(AlNO_3)_3$ were investigated; however, significant adsorption effects of specific radionuclides were not observed.

2.5 Spectroscopic Analysis

Homogenous chemical matrices cannot necessarily be analyzed using the same techniques applied to solid materials. Depending on the type of information probed, several spectroscopic analysis techniques may need to be implemented.

2.5.1 Liquid Scintillation Counting

Liquid scintillation counting is a technique commonly used to detect and determine the amount of activity that is contained within a radioactive sample, specifically alpha or beta emitters, or conversion electrons. Samples were dissolved in a known amount of scintillation "cocktail" containing an aromatic solvent and scintillants. Occasionally a second organic compound, called the waveshifter, is required in order to adsorb the photons from the primary scintillator and re-emit them at a wavelength that is easier to detect by the photomultiplier tubes (PMT). Particles emitted from the samples transfer energy to the solvent molecules in solution. These molecules then transfer their energy to the scintillants, which excite and emit light. The light that is emitted is detected by the PMTs in cpm (counts per minute). Light output for organic scintillators is slightly nonlinear, which poses problems for heavier charged particles rather than low energy emitters like ^{3}H (tritium).

Liquid scintillation counters provide ease of use as well as higher efficiencies for alpha particle radiation detection than most radiation detectors Beta particles often face photon quenching where an incomplete transfer of particle energy to solvent molecules occurs [20]. For samples used in these studies, chemical quenching also readily occurred due to the higher nitric acid concentration in samples. A 0.9 mL aliquot of water was added to the 100 μL aliquot of sample and 10 mL of Ultima Gold AB cocktail in order to reduce the acid concentration for analysis on the LSC. Spectra for samples that contained ^{90}Sr were shifted toward lower energies

due to quenching. However, the tSIE values remained high enough for each sample (maintained above 300) and the total counts were used for all data analysis within the constant region of interest (channels 1001 – 2000) . Therefore, the degree of quenching was not of concern. Coincidence time was set to 18 nsec, delay before burst was set to 75 nsec, and the static control was on for all samples counted.

A standard of known activity in dpm, disintegrations per minute, and the outputted activity in cpm, counts per minute, can be used to determine the instrument's counting efficiency using Equation 3.

$$\text{Counting Efficiency (\%)} = \frac{\text{CMP}\cdot 100}{\text{DPM}} \tag{3}$$

Where:

CPM = counts per minute

DPM = disintegrations per minute

Glass scintillation vials yield a slightly higher efficiency than plastic vials due to quenching effects in the material. Plastic vials were used in these experiments in order to reduce the potential contamination of radioactivity in the laboratories. Quenching occurs when something blocks light from being emitted. Chemical quenching takes place when another chemical competes with the primary scintillator for the excitation energy in the solvent, where as optical, or color, quenching occurs when the color within a sample causes the light outputted by the scintillator to be readsorbed. The tSIE (transformed Spectral Index of the External Standard) value can give insight as to whether a sample is quenched or not on a scale from 0 (most quenched) to 1,000 (unquenched). A standard quench calibration test can be prepared with a series of standards of constant activity and increasing quench amounts.

"Pure beta emitters" are nuclides that decay directly to the ground state of the daughter product. Liquid scintillation counters yield very broad spectra for beta emitting particles, particularly compared to sharp alpha peaks. Therefore, ^{90}Sr, a "pure beta emitter", can be difficult

to detect. For experiments where ratios are probed and only one isotope is of interest, windows or regions of interest can be set and held constant. This method isn't as efficient for activity determination, particularly when other radionuclides are present.

In order to determine the amount of activity in the ^{90}Sr standard used, an aliquot of the standard solution was taken and counted using liquid scintillation detection. An aliquot of the same size was taken from each of the samples collected from the column studies and counted by liquid scintillation counting. Each sample was counted for 60 minutes, or less if a counting uncertainty of less than two percent was obtained prior to the end of the count time. All samples counted by liquid scintillation were prepared with 10 mL of liquid scintillation cocktail, 0.9 mL of water, and 100 µL of sample. In order to mimic the sample matrix, blank samples were prepared by replacing the 100 µL of sample with water or diluted nitric acid and counted prior to and after each set of samples. The counts collected from the blanks were subtracted from each sample and used to determine and verify the background for each set of samples counted.

2.5.1.1 System Specifications and Parameters

A Perkin Elmer model 3100TR liquid scintillation counter was used to count samples containing ^{90}Sr. A counting protocol and set parameters have been set up and implemented in order to reduce counting error and optimize the liquid scintillation counting. The samples were counted for 60 minutes per sample with the count mode set to normal and the pre-count delay set to 0. The number of counts per minute for a blank sample was subtracted manually from all samples. A 2 % sigma terminator was set for samples of high amounts of activity, which reached the counting error cutoff in less than 60 minutes. Channel region, 50 through 1000, was set as the background data and channels 1001 through 2000 were representative of the sample activity.

2.5.1.2 General Counting Procedure

Samples were loaded into an empty rack, first blank, then the standard(s), and the remaining samples followed. The rack was then placed into the liquid scintillation counter and the protocol described above was applied. Upon counting completion of all samples, a report was made

available which included the counts per minute for each sample, set regions designated, the SIS quench level, and tSIE. Higher SIS and tSIE values indicate that there is little to no quenching and therefore a counting efficiency of 100% can usually be assumed. The background was subtracted from each sample using the count rate from the blank. The count rates obtained were used to determine the percent yields of radiostrontium recovered from separation schemes.

2.5.2 Gamma Spectroscopy

An HPGe, High-Purity Germanium, detector is a type of semiconductor used to determine the adsorption of photons present in a radioactive source. They consist of a depleted thickness about a few centimeters in depth, which allows for total adsorption of gamma rays up to a few MeV. Other detectors used for gamma-ray spectroscopy, i.e. NaI(Tl), often lack in resolution compared to HPGe detectors, but have high photopeak efficiencies as a compromise. HPGe detectors have the capability of seeing a photopeak above the Compton distribution much more clearly than other gamma-ray spectroscopy detectors do. A gamma emitting source will produce a recoil electron before any signal can be detected, this event can occur by one of the following three processes: photoelectric effect, Compton scattering, or pair production. The photoelectric effect implies that a gamma or x-ray will give all of its energy to the recoil electron, which in turn creates electron-hole pairs that produce an output signal to the detector. In this case all events appear as full-energy peaks in a spectrum. Through Compton scattering, a gamma ray that enters the detector and interacts with matter within the detector to produce electrons that then attenuate and eventually give off output signals. By this process, a distribution of pulse amplitudes up to a maximum pulse height, thus producing a Compton edge, occurs. A well-distributed low-energy area will be shown in the spectrum if Compton scattering occurs. When scattered photons undergo one or more additional interactions, we see complete absorption of the photons. Through pair production total absorption can also be observed, but this is not likely to occur with photons below 2 MeV. Through this process total adsorption can also be observed. Pair production occurs when a gamma ray enters the detector and creates an electron-positron pair with an initial energy

of 1.02 MeV or more (two 0.511 MeV annihilation energies). The electron will produce a pulse whose magnitude is proportional to the electron energy and the positron will produce a pulse proportional to the positron energy. The output pulse observed by the detector will be the sum of the two pulses emitted. When the positron annihilates in the detector, the gamma energies associated can escape or interact further within the detector together or one may escape and the other stay behind. Single-escape, double-escape, and/or full-energy peaks can represent these events.

Figure 14 below represents the likelihood of photoelectric, Compton, or pair production occurring in a given source within a semiconductor detector. Total absorption can also be observed through the gamma emission process of pair production.

Another method of nuclear decay is electron capture, where an orbital electron, often a K-electron, straying too close to the nucleus gets captured and a proton is converted into a neutron. The resulting atom has the desired number of orbital electrons; however, a vacancy in one of the inner shells occurs. Once the vacancy is filled, X-rays are then generated and are characteristic of the product element. The decay can populate the ground state of the product nucleus or it can occupy the excited state so that gamma rays from subsequent nuclear de-excitation may occur in addition to characteristic X-rays. In the electron capture of ^{85}Sr, one of its electrons combines with a proton in the nucleus to form a neutron, and a gamma particle of 0.514 MeV gets expended in the process.

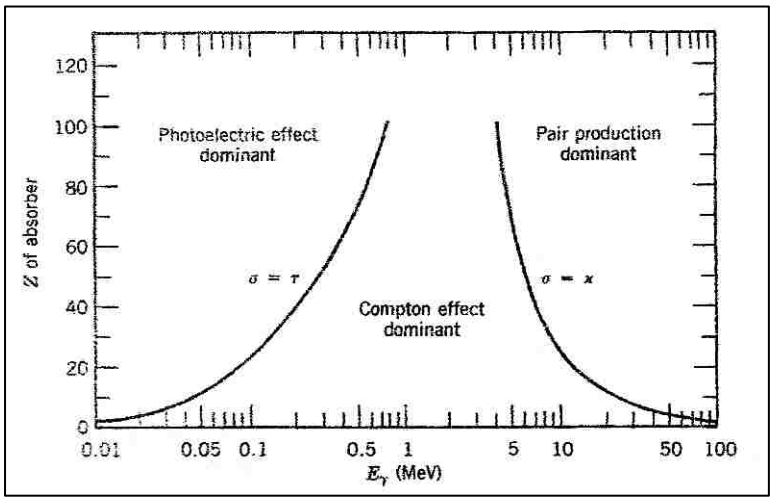

Figure 14 The three γ-ray interaction processes and their regions of dominance. Krane[21]

2.5.2.1 System Specifications and Parameters

An HPGe (High-Purity Germanium) detector along with the Genie 2000 software from Canberra was used to count samples containing ^{85}Sr. The spectrometer was calibrated using an^{125}Sb and ^{152}Eu standardwith photopeaks including the following energies: 463.36 keV and 600.60 keV. A range of 60 channels was held constant from windows 2447 to 2507 for the ^{85}Sr photopeak of 514 keV. Each sample was counted for 3 hours in order to reduce counting error and optimize sample resolution. A well detector was used for roughly twenty remaining samples towards the end of the studies when much of the ^{85}Sr had already decayed. The well detector covers more of the sample than the original HPGe detector used, thus allowing for equivalent counting statistics for samples with lower activity.

Figure 15 HPGe with liquid nitrogen Dewar

2.5.2.2 General Counting Procedure

Samples from the batch studies were filtered and then 0.9 mL of the filtered solution was transferred to an empty 5 mL conical tube and diluted to 1.0 mL with 4M nitric acid. The conical tubes were placed inside the detector into a fitted sample holder and counted for three hours. The total counts under the ^{85}Sr 514 keV peak were recorded and a blank that was counted prior to sample counting was subtracted and the samples were then compared to the standard, which was run prior to the samples. The counts obtained from the areas of a fixed channel region were saved and used for the calculation of the k' values, or resin capacity factors. All concentrations were run in replicates of five for each concentration and/or under each condition throughout the entire batch distribution studies.

The column studies yielded three fractions: load, rinse, and strip. For each sample containing ^{85}Sr, 1.0 mL of each fraction was transferred to an empty tube and counted on the gamma spectrometer for three hours. The total counts under the 514 keV peak were recorded, and a blank

that was counted prior to sample counting was subtracted from each sample individually and then compared to the standard that was representative of the sample matrix. All samples were in nitric acid media and a consistent geometry was used. The counts were collected from the same window region of set channel numbers and used to calculate the recovery values for radiostrontium.

2.5.2.3 Efficiency

An efficiency calibration was not needed since the samples were referenced to a common standard.

2.5.3 Inductively Coupled Plasma – Atomic Emission Spectroscopy

Figure 16 Inductively Coupled Plasma - Atomic Emission Spectroscopy

2.5.3.1 System Specifications and Parameters

Samples are introduced into the ICP-AES through the peristaltic pump and then carried to the nebulizer, where Argon gas aids in the conversion of the sample into a mist. About 1% of the mist is transported to the torch and the remaining particles exit as waste. Argon gas excites the electrons of the mist from the torch to the plasma where the analytes of the sample emit a characteristic wavelength, which is used to detect analytes.

2.5.3.2 General Procedure

In general, samples should be diluted with roughly 1% nitric acid and should be in the range of 1 ppm to 100 ppm in order to be analyzed by ICP-AES. For most metals with concentrations between 0.1 M and 2.0 M a 1:1,000 dilution should be performed and a 1:10,000 dilution for samples greater than 2.0 M. Samples were placed into an automated sample tray, beginning with the blank and then up to 6 standards, followed by the samples. An automated protocol was set up so that the blank and the standards were run first, the tubes were rinsed for thirty seconds before and after each sample, and specified wavelengths of interest were observed. The software allowed for each sample to be analyzed three times sequentially. After all of the samples were counted, the data was transferred into an excel data sheet, where the blank was subtracted from all of the standards and samples. The standards were used to determine the system LOD, limit of detection, and were compared to the samples. Three vials were prepared identically for each sample observed.

ICP standards were used to verify the linearity of the ICP-AES measurements for aluminum, calcium, magnesium, phosphorous, potassium, and zirconium as well as determine the Minimum Detectable Limit (MDL) for the instrument. A blank with 1% nitric acid was prepared as well as five standards. Al, Ca, K, Mg and Zr standards of 1, 5, 10, 50, and 100 ppm and P standards of 0.33, 0.36, 16.3, 32.6, and 65.2 ppm were used. Three aliquots were taken from each sample, analyzed, and then averaged. The data was used to determine the lowest concentrations detectable by the ICP-AES for each metal ion. The MDL for each metal ion was calculated using Equation 4 below and the following concentrations: 1 ppm [Al^{3+}], 0.01 ppm [Ca^{2+}], 0.8 ppm [K^{+}], 0.05 ppm [Mg^{2+}], 0.33 ppm [P^{5+}], 0.1 ppm [Zr^{4+}].

$$MDL = \frac{Stdev \cdot t \cdot concentration}{average} \quad (4)$$

Where:

t = 3.14

Stdev = standard deviation

Table 1 lists the average minimal detectable limit of the select metal ions as well as the relative standard deviation of each set of samples associated.

Table 1 ICP-AES minimum detectable limits

Element	MDL	RSD
Al	0.055 ppm	1.75%
Ca	0.003 ppm	9.12%
K	0.034 ppm	1.34%
Mg	0.003 ppm	1.64%
P	0.039 ppm	3.72%
Zr	0.014 ppm	4.54%

Standards used for the batch studies included aluminum nitrate from BDH ARISTAR PLUS, calcium nitrate SRM3109a from NIST, potassium nitrate from CPI International, magnesium nitrate from Environmental Resource Associates, phosphate traceable to NIST SRM 3186 from ERA The Industry Standard Cal, and zirconium (IV) fluoride from Alfa Aesar. Standards used for the column studies included calcium nitrate and magnesium nitrate from SPEX Certiprep and strontium nitrate from Assurance.

2.6 Materials

A list of materials used for all experiments can be found in appendix II.

2.7 Objective of Research

While many methods exist to separate and analyze radionuclides within environmental matrices, the performance of all of these methods is limited by interfering constituents that are found in most environmental samples. The presence of these particulates can significantly reduce the recovery of the radiostrontium and lead to incomplete separations. The goal of this work is to determine the major and minor constituents present in various samples of bone, and to determine their influence on current method performance and strontium recovery (i.e. extraction chromatography). In addition, the basic chemistry that plays a role during the separation is probed.

CHAPTER 3

3 RESULTS

3.1 Data Analysis

3.1.1 X-ray Powder Diffraction

Bone ash samples were characterized by XRD and SEM prior to dissolution. The XRD results are shown below in Figure 17 for the five bone samples used in the column distribution studies. The patterns of bone from left to right are as follows: IAEA-12, NIST 4356, NIST 1400, Ebonex, and Lake Mead. All of the samples were determined to be predominantly hydroxyapatite except for small contaminants observed in the NIST 1400, Ebonex, and Lake Mead samples. The NIST 1400 bone sample contained a sodium carbonate magnesium phosphate contaminant. The Ebonex sample contained a small amount of periclase, or magnesium oxide, and the Lake Mead sample contained a minute quantity of corundum, aluminum oxide.

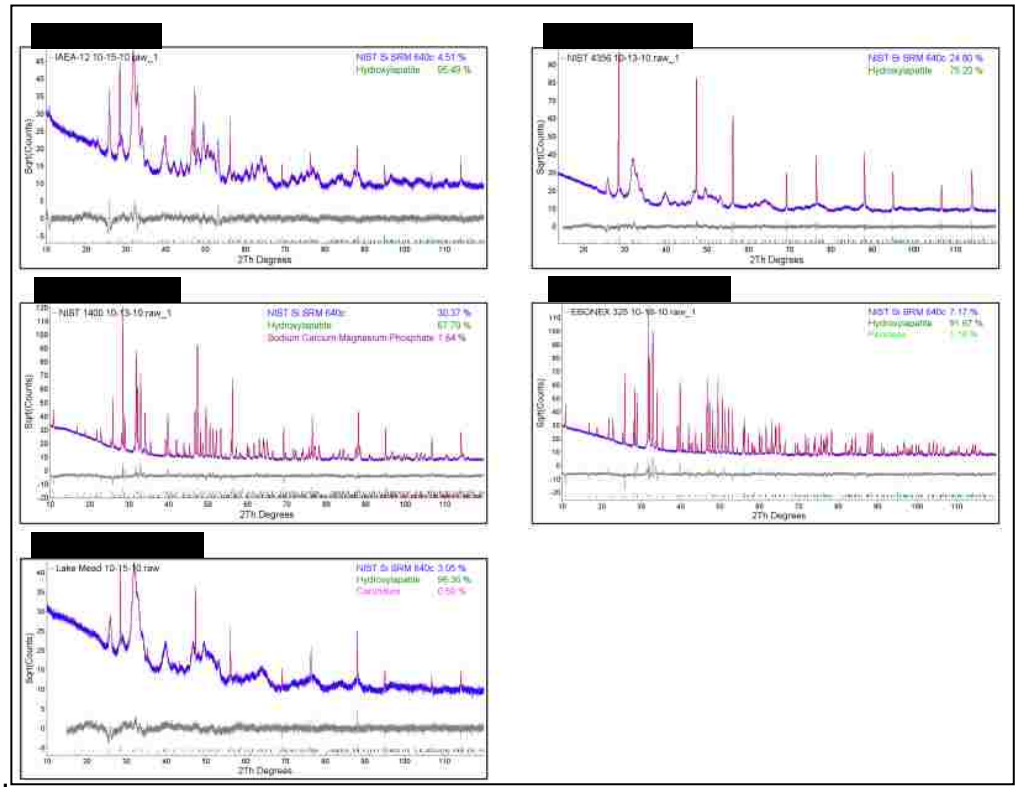

Figure 17 X-ray Powder Diffraction patterns for various bone samples

3.1.2 Scanning Electron Microscopy

A JEOL Scanning Electron Microscope model JSM-5610 accompanied by a backscattered electron (BE) and secondary electron (SE) detector, as well as an EDS (energy dispersive spectrometer) was used to characterize bone materials with respect to their morphology and to determine the elemental makeup of the samples. General surface structure, minor contaminants, and calcium to phosphorous ratios were probed. Figure 18 shows some of the images obtained for the five samples using SEM.

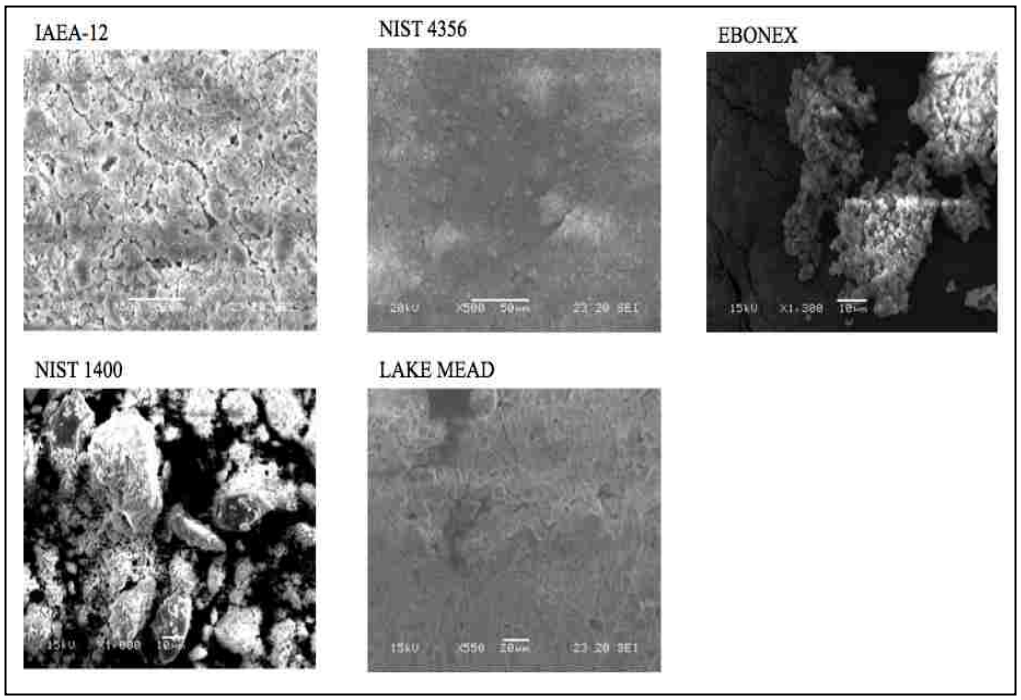

Figure 18 Scanning Electron Microscopy images of various bone samples

Table 2 shows contaminants found in each bone sample using SEM. The ratios of the percentages are not completely representative of the entire samples, but rather indicate of several local regions of the sample analyzed**.**

Table 2 SEM composition of bone samples

IAEA-12								
	Au	Ca		Mg		O	P	
	1.55%	22.02%		0.38%		63.75%	12.50%	
NIST-4356								
Al	Au	Ca				O	P	
1.06%	1.12%	22.51%				61.21%	14.10%	
EBONEX								
Al		Ca	K	Mg	Na		P	Si
8.62%		22.12%	1.76%	0.83%	0.59%		13.54%	7.04%
NIST 1400								
	Au	Ca		Mg	Na	O	P	
	2.23%	44.98%		0.89%	0.62%	29.08%	19.03%	
LAKE MEAD								
	Au	Ca				O	P	
	1.29%	18.46%				69.48%	10.79%	

3.2 Batch Distribution Studies

3.2.1 Inductively Couple Plasma –Atomic Emissions Spectroscopy

Ion solutions used in the batch studies were analyzed by the ICP-AES in order to determine the actual concentrations of elements present. Two samples of each concentration were run, and each sample was analyzed in replicates of three. The calculated concentrations were replaced in the batch studies trends with the experimentally determined values shown in Table 3. All of the measured values reasonably agree with the calculated concentrations except for Zirconium, due to the difficulty in forming homogenous mixtures.

Table 3 Concentrations of ion solutions used in batch studies

Element	Calculated Value	Actual Value	Standard Deviation
Al			
	0.1	0.09	1.5E-04
	0.3	0.26	1.4E-04
	0.5	0.43	2.1E-05
	1.0	0.92	1.4E-04
	1.5	1.33	3.1E-05
	3.0	2.77	1.8E-05
Ca			
	0.1	0.08	4.8E-06
	0.2	0.17	2.3E-06
	0.3	0.25	1.7E-06
	0.4	0.34	1.3E-06
	0.5	0.43	2.1E-06
	1.0	0.81	1.1E-06
	2.5	2.17	9.7E-07
K			
	0.1	0.09	1.9E-05
	0.2	0.19	3.1E-05
	0.3	0.29	4.6E-05
	0.4	0.38	4.6E-03
	0.5	0.47	2.7E-05
	1.0	0.92	2.1E-05
	2.0	1.54	6.7E-06
	3.0	2.02	4.0E-05
	4.0	2.87	7.8E-06
	5.3	4.10	4.6E-05
K - PO_4			
	0.1	0.09	1.5E-02
	0.3	0.25	4.5E-05
	0.5	0.43	2.0E-05
	0.7	0.58	5.4E-05
	1.0	0.88	3.9E-05
	2.0	1.67	3.2E-05
	3.0	2.50	1.0E-05
	3.5	2.79	7.8E-06
Mg			
	0.1	0.09	6.1E-06
	0.3	0.34	2.1E-06
	0.5	0.59	2.7E-06
	1.0	1.11	1.7E-06
	4.0	5.23	4.1E-06
Zr			
	0.1	0.00	5.4E-05
	0.3	0.08	3.0E-05
	0.5	0.19	1.1E-06
	1.0	0.10	1.6E-05

3.2.2 Mass and Kinetic Studies

A mass study of 50 mg of SR resin compared to that of 75 mg of resin was conducted using ^{85}Sr in nitric acid and counted using gamma spectroscopy. The results from Table 4 show that the calculated resin capacity factor, k', was independent of the mass of the resin used, as predicted.

Table 4 Resin capacity factor, k' [11]

	Average k'	
50 mg SR Resin	14.89	± 0.47
75 mg SR Resin	14.60	± 0.26

A separate kinetic study was performed to determine the amount of time required to reach a state of equilibrium between the radiostrontium and the SR resin, as well as to ensure all parts were thoroughly mixed. The contact times observed included 1 hour, 6 hours, and 24 hours. The results of the study shown in Figure 19 assured state of equilibrium reached after one hour of mixing using 50 mg of resin.

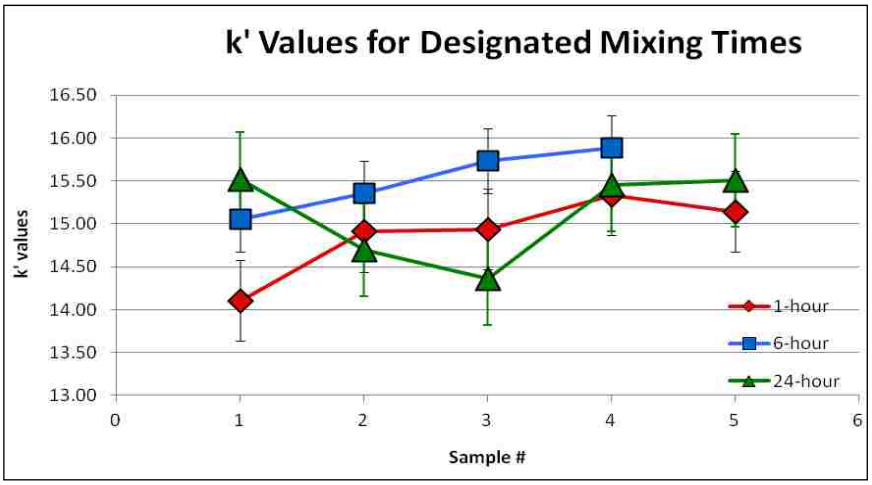

Figure 19 Average k' values for mixing times of 1 hour, 6 hours, and 24 hours of 50 mg of SR resin

3.2.3 Gamma Spectroscopy Recovery Yields

Calcium bromide salt dissolved and diluted in 4 M nitric acid was used to observe the elemental effects of calcium. Five replicates of each concentration of 0.08, 0.17, 0.25, 0.34, 0.43, 0.81, and 2.17 M calcium [2^{+}], verified by ICP-AES, were analyzed as well as a blank. The results shown

in Figure 20 suggest that calcium inhibits the sorption of ^{85}Sr to SR resin removed from 2 mL pre-packed Eichrom cartridges at concentrations somewhere between 0.1 and 0.5 M. The affinity for strontium on to the SR resin gradually increases beyond 0.5 M at least until 2.17 M calcium [2^+].

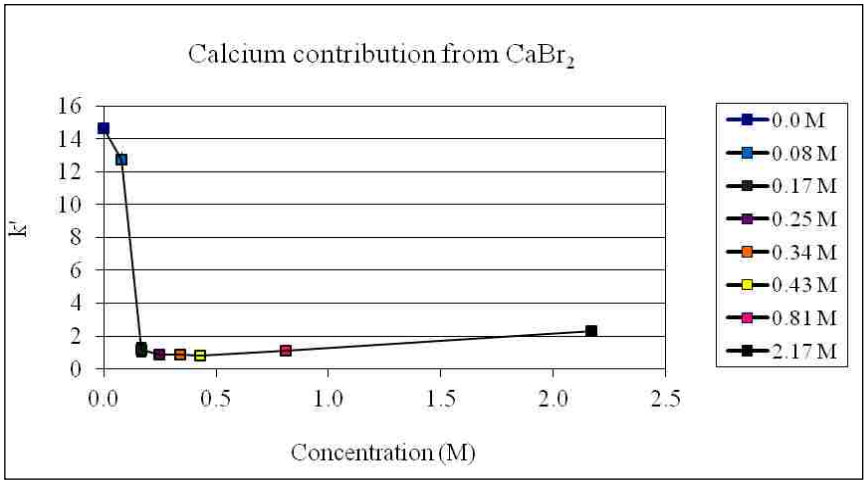

Figure 20 Contribution of calcium [2+] on the separation of radiostrontium from calcium bromide

Elemental effects from potassium and/or phosphate were observed using a potassium phosphate salt dissolved in 4 M nitric acid. A blank, as well as five replicates of each concentration of 0.09, 0.25, 0.43, 0.58, 0.88, 1.67, 2.50, and 2.79 M potassium [1^+] and phosphate [1^-], verified by ICP-AES, were observed. Results, or k' value trends, represented in Figure 21 suggest that either the potassium or phosphates are responsible for the immediate decrease in sorption of ^{85}Sr to the SR resin removed from 2 mL pre-packed Eichrom cartridges from 0 M to at least 2.79 M potassium [1^+].

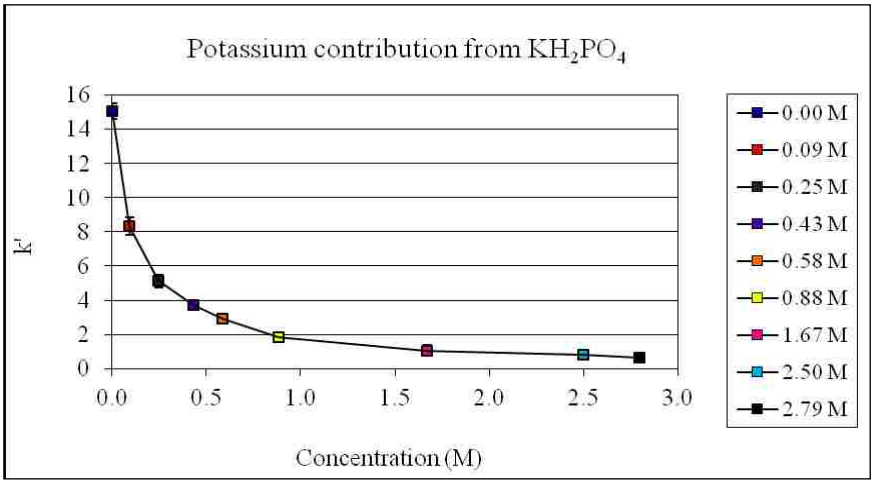

Figure 21 Contribution of potassium [1+] and/or phosphate on the separation of radiostrontium from monopotassium phosphate

The SR resin used for the two studies, shown in Figure 21 and 22, came from 2 mL pre-packed cartridges, whereas the remaining studies, shown below, utilized loose SR resin. Thus yielding a noticeable different in the k' values; although the trends remain the same regardless of the resin used.

In order to determine whether or not the contributions towards the uptake of strontium onto the SR resin was due entirely upon the potassium ion or the phosphates, another set of solutions were prepared and analyzed using potassium bromide: 0.09, 0.19, 0.29, 0.38, 0.47, 0.92, 1.54, 2.02, 2.87, and 4.10 M potassium [1^+], and verified by ICP-AES, with 4 M nitric acid. Figure 22 suggests that potassium, when in the absence of phosphate, rapidly reduces the affinity of radiostrontium to the SR resin until the affinity is virtually non-existent at 0.5 M K [1^+].

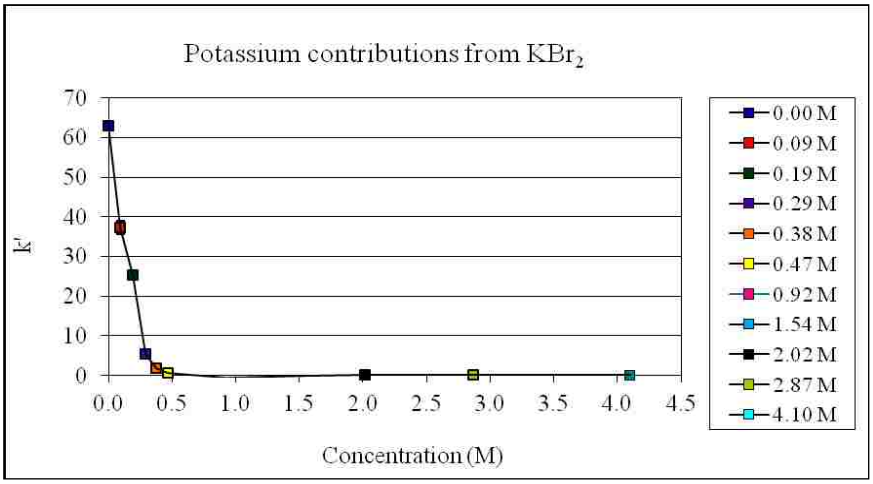

Figure 22 Contribution of potassium [1+] on the separation of radiostrontium from potassium bromide

Elemental contributions from magnesium [2^+] were also observed using a magnesium bromide salt dissolved in 4 M nitric acid. Concentrations of magnesium included 0.09, 0.19, 0.29, 0.38, 0.47, 0.92, 1.54, 2.02, 2.87, and 4.10 M. Figure 23 suggests that magnesium rapidly reduces the affinity of radiostrontium to the SR resin until 0.59 M magnesium [2^+], at which point the affinity becomes preferential. As the matrix concentration of magnesium increases from 1.11 M magnesium [2^+], the resin capacity factor value surpasses the value of the standard by 5.3 M.

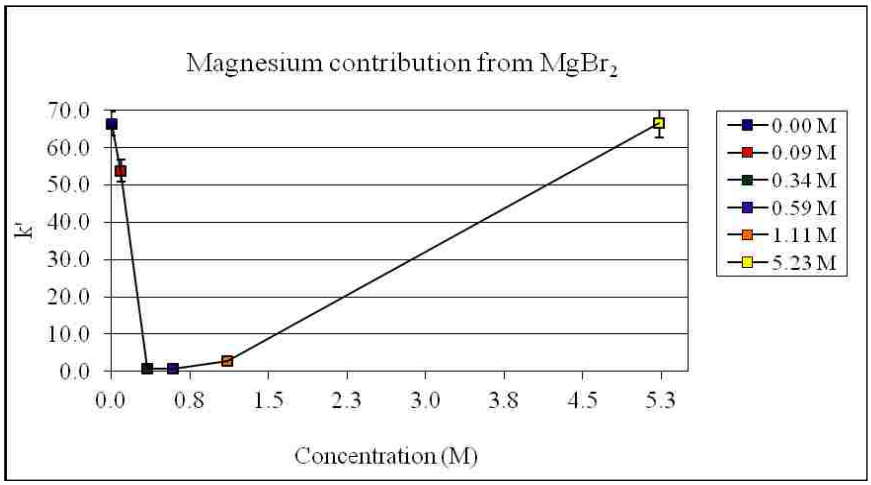

Figure 23 Contribution of magnesium [2+] on the separation of radiostrontium from magnesium bromide

The elemental contributions from aluminum [3^+] were observed using aluminum trichloride dissolved in 4 M nitric acid. Concentrations 0.09, 0.26, 0.43, 0.92, 1.33, and 2.77 M aluminum [3^+], shown in Figure 24, propose synergism between aluminum and radiostrontium onto Sr-specific resin.

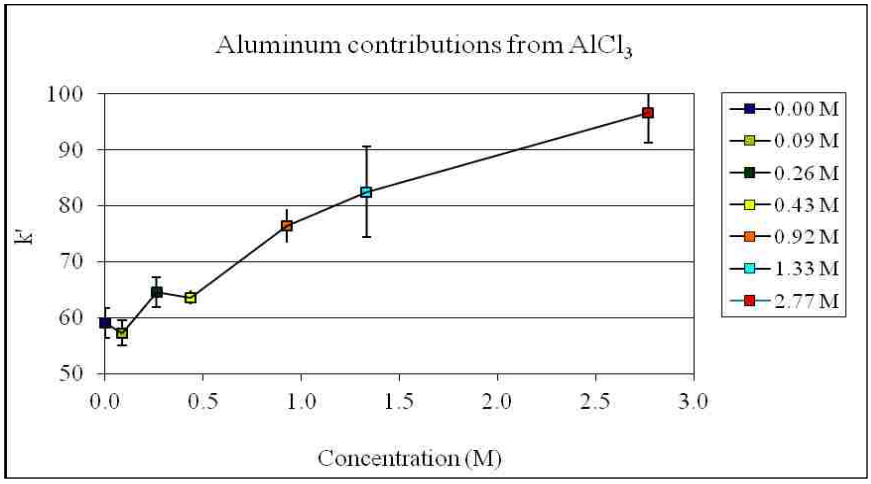

Figure 24 Contribution of aluminum [3+] on the separation of radiostrontium from aluminum chloride

Zirconium (IV) sulfate crystals were dissolved in 4 M nitric acid to obtain concentrations of 0.003, 0.079, 0.102, and 0.195 M zirconium [4^+]. From the results shown in Figure 25, zirconium seems to play no role in the adsorption of radiostrontium onto the Sr-specific resin; at least from the limited range of 0.003 to 0.102 M zirconium [4+]

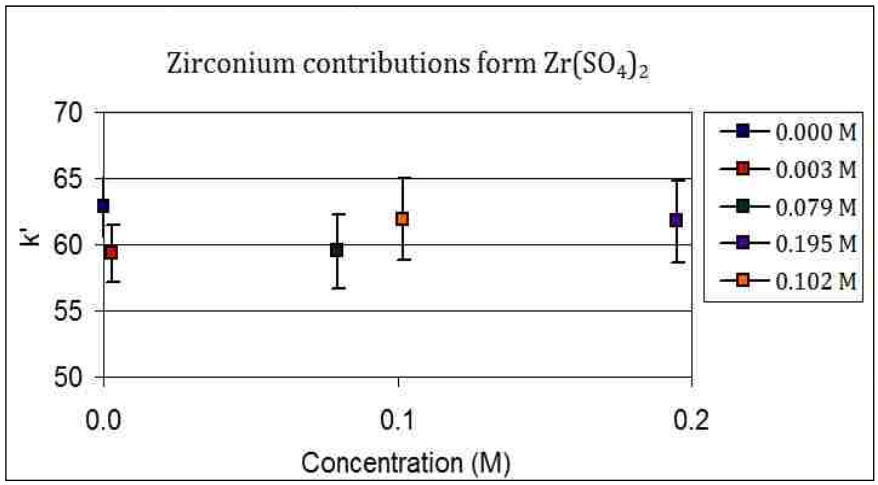

Figure 25 Contribution of zirconium [4+] on the separation of radiostrontium from zirconium (IV) sulfate

3.3 Column Separation Studies

The role of major bone components, calcium and phosphate, on the separation method of radiostrontium using Sr-specific resin were observed using more industrial techniques. Minor contaminants of bone were present in the matrices and allowed to contribute to the separation scheme.

3.3.1 Recovery Yields

^{90}Sr was separated and counted to ensure method validation compared to current similar techniques. The separations of ^{90}Sr with SR resin were performed at various pressure settings in order to determine the optimal experimental conditions for the highest recovery yields. Radiostrontium was isolated at vacuum pressure settings of 650, 675, and 690 torr. LSC data were used to determine the percent recovery of the ^{90}Sr. As shown in Figure 26, a pressure of 675 torr appeared to give the best recovery rates. The average flow rate for 650 torr was 1.30 ± 0.39 mL min^{-1}, 1.10 ± 0.17 mL min^{-1} for 675 torr, and 0.49 ± 0.14 mL min^{-1} for 690 torr.

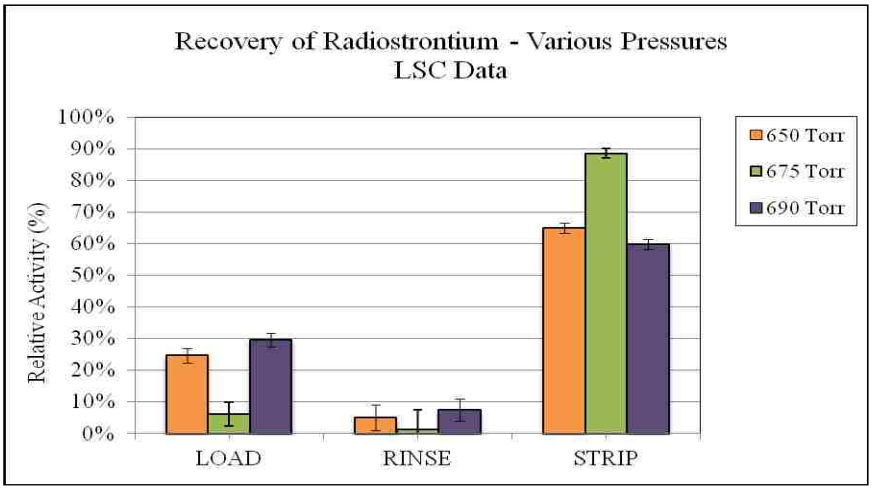

Figure 26 Recovery of radiostrontium at various pressure settings

The pressure setting of 675 torr was chosen as the optimal setting for the column studies, because it is still close to ambient conditions and has appeared to give forth a strontium yield comparable to that published in the literature [1] The average flow rate for a load solution of 5 mL

was 0.75 ± 0.20 mL min^{-1} and 1.08 ± 0.25 mL min^{-1} for load solutions of 6 mL. The fractions collected from the load, rinse, and strip phases were counted by LSC within an hour after the separations were performed. Each fraction was analyzed again days later to account for the in-growth of ^{90}Y. The data was collected and used to determine relative recovery yields of ^{90}Sr. The change of counts over time starting from the initial point of separation up to a few months later is shown in Figure 27 for 0.1 M Ca^{2+} generic bone ash, purchased from Ebonex.

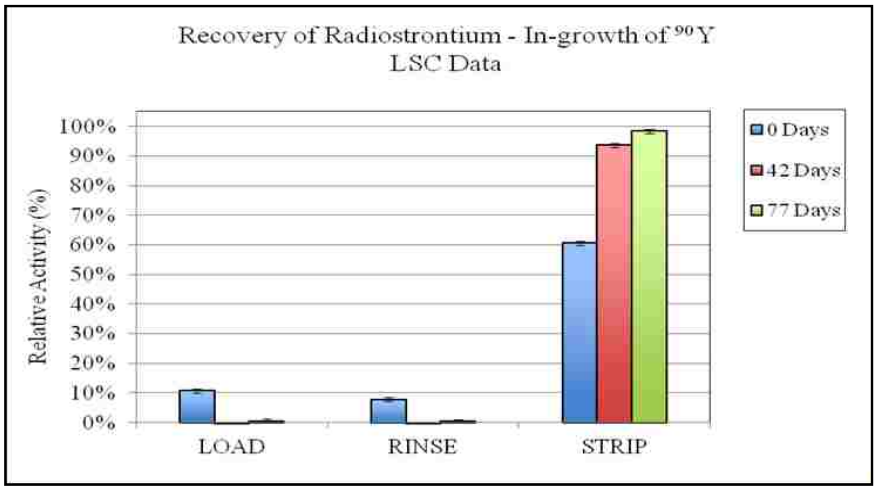

Figure 27 Recovery of radiostrontium in the presence of 0.1 M Ebonex bone ash using the in-growth of ^{90}Y

Fractions collected from the column separations studies were also analyzed using ICP-AES as an additional attempt to verify which fractions elemental strontium and calcium were eluted. Figure 28 shows the percent recovery of elemental calcium that elutes during the load, rinse, and strip fractions of three varying bone materials, but in specified calcium matrix concentrations. It appears that matrices containing lower concentrations of calcium, such as 0.1 M and/or 0.4 M, and fewer contaminants, magnesium (0.89%) and sodium (0.62%), elute more calcium during the load phase and very little to none during the strip phase. However, for samples of 0.8 M calcium [2^{+}] concentrations and a larger amount of contaminants, such as aluminum (8.62%), magnesium (0.83%), potassium (1.76%), silicon (7.04%), and sodium (0.59%) a reduced amount of elemental calcium is shown to be eluted during the load phase and a statistically larger probability of

calcium breakthrough in the strip fraction is observed. For increasing concentrations of calcium, a greater amount of calcium is shown to be eluted in the rinse phase.

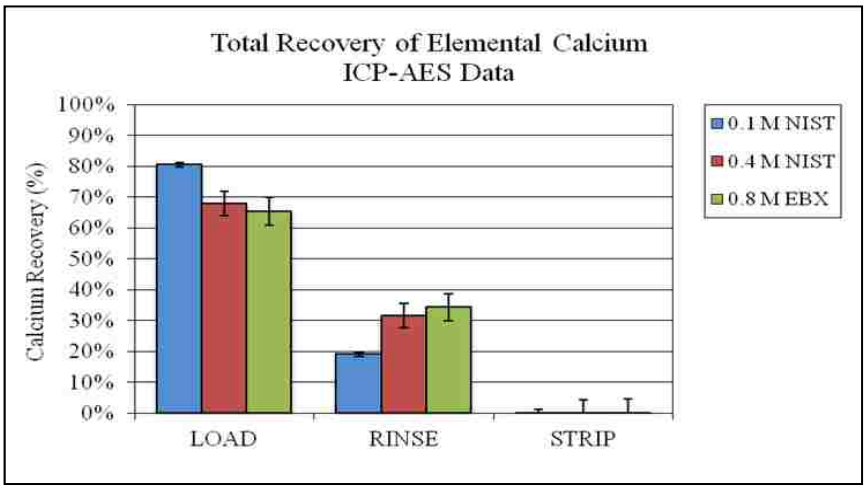

Figure 28 Total recovery of elemental calcium for selected bone ash matrices

For the same set of sample matrices, Figure 29 shows percent recoveries for elemental strontium from the load, rinse, and strip fractions. Primarily all of the strontium is eluted with the strip fraction for the three samples containing calcium concentrations between 0.1 M and 0.8 M. A small fraction of elemental strontium is shown to breakthrough the column during the rinse phase for the generic bone ash sample containing the largest concentration of calcium and contaminants.

These results also verified that the lower strontium recovery yields obtained from the original LSC data was in fact due mainly to the contribution of ^{90}Sr and the in-growing ^{90}Y.

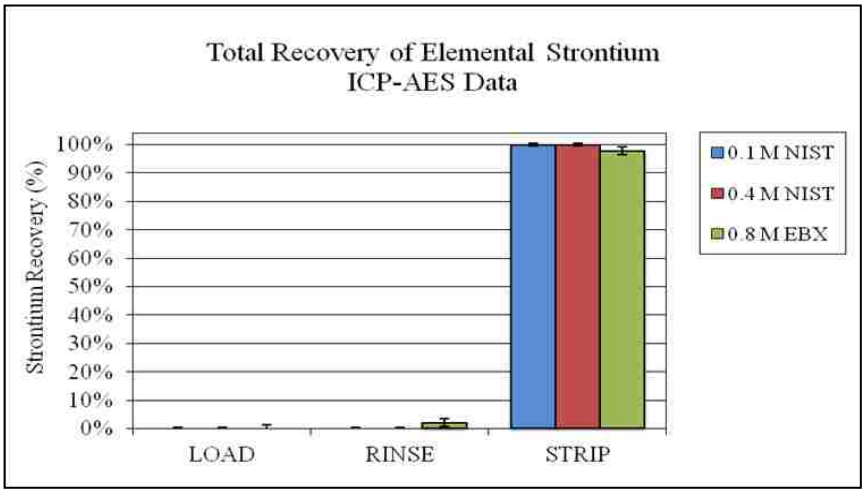

Figure 29 Total recovery of elemental strontium for selected bone ash matrices

Strontium-90 is a pure-beta emitter, with a very broad peak spectrum, and is also subjected to peak shifting; therefore a tracer of ^{85}Sr was added to the load solution and used to verify percent recoveries of radiostrontium using SR resin. The volume in each phase increased from 5 mL to 6 mL to accommodate the additional material added. The solutions were loaded onto a SR resin column and later collected with the strip fraction. Figures 30, 31, and 33 represent data obtained from the gamma spectrometer for analysis of tracer ^{85}Sr. Samples in Figures 31 – 33were prepared by dissolving 3.3 grams of bone ash in a final 25 mL of 4 M nitric acid solution so that they could be compared directly by mass at a higher concentration of calcium for all sample types. Each sample contained both ^{85}Sr and ^{90}Sr; therefore, fractions from each separation were collected and able to be analyzed on LSC, gamma spectroscopy, and ICP-AES (Figures 28 and 29).

For the separation of radiostrontium in the presence of NIST certified bone ash, concentrations of 0.1, 0.4, 0.6, and 0.8 M calcium [2^+] and 0.8 M calcium [2^+] of a generic bone ash, purchased from Ebonex Corporation, were observed and the results can be shown in Figure 30. It appears that the sample containing the lowest concentration of calcium actually has the lowest recovery of radiostrontium; however, when taking error into consideration, all of the

samples behaved similarly Elemental calcium and strontium results from ICP-AES can be seen in Figures 28 and 29 for three of the five samples here.

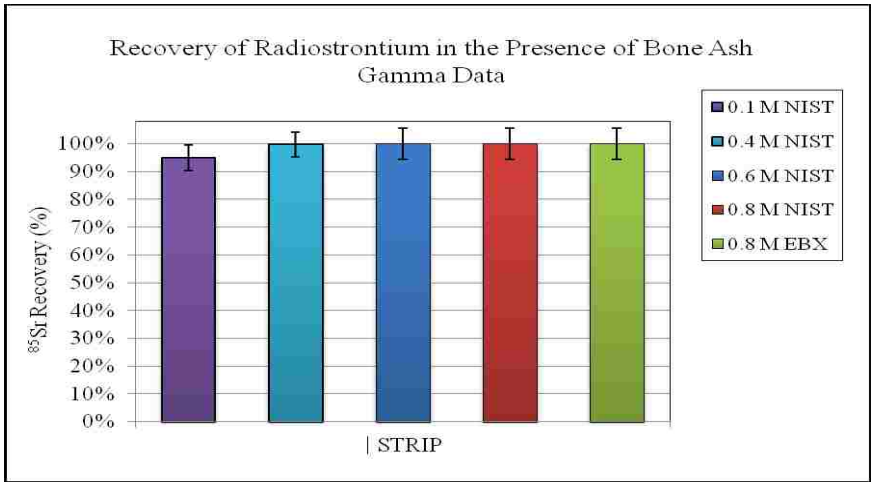

Figure 30 Recovery of radiostrontium in the presence of various concentrations of bone ash

Figure 31 directly compares an IAEA-12, NIST 4356, and NIST 1400 certified bone ash standard, as well as a generic sample obtained from Ebonex by identical mass. The samples were prepared by mass of ashed bone; since actual mesh size varied as well as the minor contaminants, the effects on these recoveries could be from any number of contributions. However, one noteworthy feature to point out would be the small spike of radiostrontium incorporated in the IAEA-12 and NIST 4356 standards and not in the lower recovery samples of standard NIST 1400 and generic Ebonex of 325 mesh; although, the spikes did not make much of a difference in the final recovery of radiostrontium.

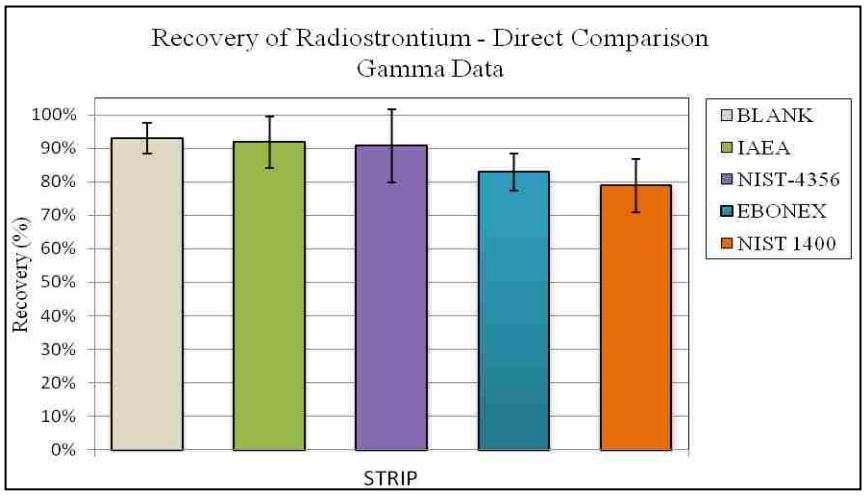

Figure 31 Recovery of radiostrontium in the presence of various bone ash matrices made up of 3.3 g bone ash and dissolved to a total volume of 25 mL and a concentration of 4 M nitric acid

Figure 32 exhibits the LSC results from a direct mass comparison of a NIST certified sample, a generic sample from Ebonex, and an environmental bighorn sheep sample from Lake Mead, Nevada, which each sample consisted of 3.3 grams of bone ash dissolved in a final volume of 25 mL of 4 M nitric acid. The environmental sample appears to yield a better recovery of radiostrontium than the two certified bone ash standards.

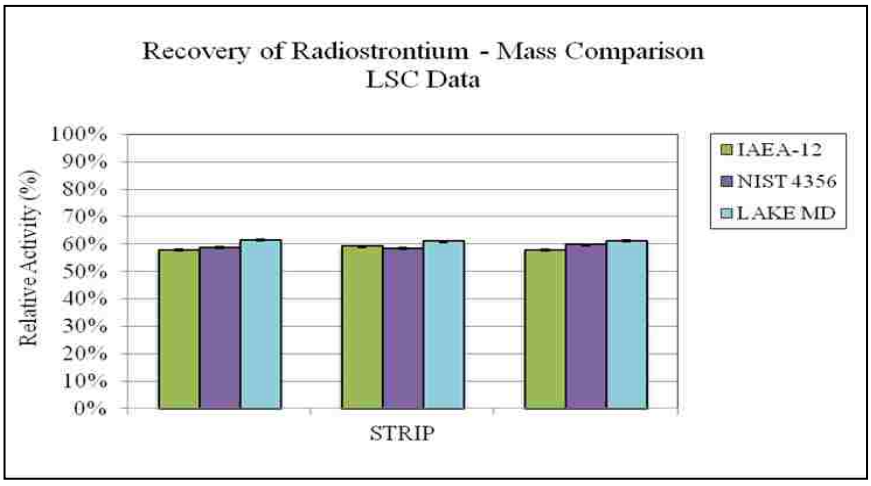

Figure 32 Recovery of radiostrontium in the presence of various bone ash matrices made up of 3.3 g bone ash and dissolved to a total volume of 25 mL and a concentration of 4 M nitric acid

Figure 33 represents the recovery of ^{85}Sr located in the same fractions analyzed in samples depicted in Figure 32, which samples exhibit the direct mass comparison of a NIST certified

sample, a generic sample from Ebonex, and an environmental bighorn sheep sample from Lake Mead, Nevada using 3.3 grams of bone ash dissolved in a final volume of 25 mL of 4 M nitric acid. Taking the range of error into consideration, the environmental sample indicates a slightly better recovery of radiostrontium; .

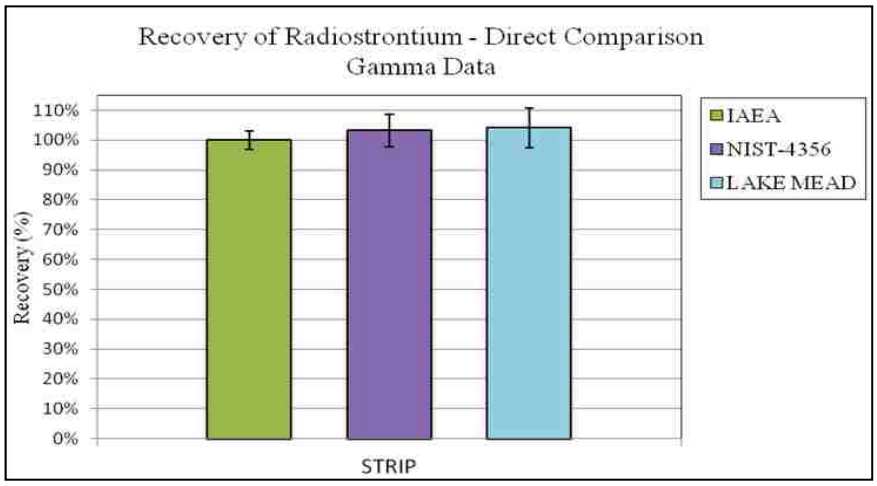

Figure 33 Recovery of radiostrontium in the presence of various bone ash matrices made up of 3.3 g bone ash and dissolved to a total volume of 25 mL and a concentration of 4 M nitric acid

3.3.2 Matrix Influences

The column studies allow for samples of fixed calcium concentrations to be analyzed; however, the addition of strontium and nitric acid cause the calcium concentration to be diluted; this effect is solved by consistent load and rinse volumes. Also, minor constituents as well as the variability of large concentrations of phosphate can be found in each sample. Thus, elemental matrix effects can be better understood by the batch experiments, particularly due to the closeness of data values and associated errors obtained from the column experiments.

CHAPTER 4

4 DISCUSSION

4.1 Non-destructive Sample Analysis

Various bone ash materials were characterized by Scanning Electron Microscopy and X-ray Powder Diffraction techniques. The XRD patterns were used to verify the composition of all of the bone ash matrices used in this work. Both certified NIST samples (1400 and 4356), certified IAEA-12 sample, generic Ebonex sample, and the environmental bighorn sheep sample from Lake Mead all predominantly consisted of hydroxyapetite, or bone. The NIST 1400 sample contained a small amount of Sodium Calcium Magnesium Phosphate, which may be a contaminant or additive, the Lake Mead sample contained corundum, or aluminum oxide, which was incorporated into the sample when the bone was crushed in-house, and the Ebonex sample contained periclase, or magnesium oxide, which may also either be contaminant or an additive during the preparation process. SEM was utilized to provide detailed images of the bone material at a microscopic level as well as to obtain an estimate of material contaminants. Each sample contained gold due to the thin gold layer of gold that was coated onto the sample in order to allow for conductivity. The content of gold per sample varied due to possible uneven coating; therefore, percentages should not necessarily be accepted as actual percent values for the entire sample, but rather just for the select regions elected and imaged. The calcium to phosphate ratios ranged from 1.60 to 2.36. All samples, except for the Lake Mead sample, contained other elemental contaminants, which included magnesium, aluminum, potassium, and sodium. Batch distribution studies were subsequently used successfully to probe the effects of most of these major and minor constituents identical of bone.

4.2 Batch Distribution Studies

The batch distribution studies proved to be an invaluable tool to evaluate the effects of common environmental elements present in bone ash on the adsorption of radiostrontium onto SR resin from Eichrom technologies. The use of gamma spectroscopy and ^{85}Sr as a tracer allowed for the rapid detection of strontium and the observation of adsorption trends in the presence of each potentially interfering element. An ^{125}Sb and ^{152}Eu standard was used in order to calibrate the gamma spectrometer for counting samples containing ^{85}Sr. Ions of interest included calcium, magnesium, aluminum, potassium, phosphate, and zirconium, most of which have been found to be common contaminants of bone.

Calcium, using a calcium bromide solution in nitric acid, predominantly responsible for the makeup of bone, was studied from concentrations of 0 M up to 2.17 M [Ca^{2+}]. A negative effect on the sorption of radiostrontium onto the SR resin was revealed beginning at concentrations as low as 0.08 M [Ca^{2+}].

The contributions from potassium were observed when in the presence of phosphate, a major component of bone, and in the absence of phosphate to simultaneously elucidate the effect of the phosphate counter ion. In the absence of phosphate, using a potassium bromide solution in nitric acid, concentrations up to 4.10 M [K^{+}] were investigated. The affinity of radiostrontium to the SR resin decreased beginning at 0.09 M potassium [1^{+}] until 0.5 M, where there was virtually no attraction to the resin. The average k' of 62.85 ± 2.25 was observed for the standard and for concentrations of 0.5 M up to 4.10 [K^{+}], k' values were averaged 0.07 ± 0.36. When in the presence of phosphate, using a potassium phosphate solution in nitric acid, concentrations up to 2.79 M [K^{+}] were observed to cause a reduction in the adsorption of strontium onto the SR resin; however, it was much more gradual. An initial k' value of a radiostrontium standard without any elemental contributors was observed at the k' of 15.04 ± 0.47 and following the increase in concentration of the potassium a final k' value of 0.67 ± 0.15 was observed for 2.79 M. The k'

scales vary due to the batch of resin used, either older resin removed from 2 mL pre-packed cartridges or newer loose resin; however the trends are comparable.

The effects of aluminum on the adsorption of radiostrontium onto SR resin were analyzed using an aluminum chloride solution in nitric acid. Concentrations of 0 M to 2.77 M [Al^{3+}] demonstrated significant enhancement, an increase in value of almost a factor of two was observed from 0 M up to 2.77 M aluminum [3^{+}], or a synergistic effect in the sorption of ^{85}Sr with increasing concentration.

The sorption of radiostrontium when in the presence of magnesium, using magnesium bromide in nitric acid, varied greatly. Concentrations of 0 M up to 5.23 M [Mg^{2+}] were studied. Strontium's affinity to the resin dropped from a k' value of 62.94 ± 2.25 to 0.75 ± 0.16 at 0.34 M [Mg^{2+}] and began to increase again at a concentration of 0.7 M [Mg^{2+}] up to 5.23 M [Mg^{2+}], where the affinity surpassed the blank at a k' value of 66.59 ± 3.90.

Although zirconium was not found to be a common habitant of bone, it is however found as a fission product in many environmental samples of interest; concentrations up to 0.195 M [Zr^{4+}] were investigated using a zirconium (IV) sulfate solution in a final 4M nitric acid matrix. Zirconium appeared to have no effects on the sorption of radiostrontium onto SR resin.

4.3 Column Separation Studies

The vacuum box used for the column separations of radiostrontium was held at a set pressure of 675 torr with an average flow rate of 0.75 ± 0.20 mL min^{-1}, which was found to be most optimal based on the higher relative activity percentages for that of 650 torr and 690 torr, for all separations conducted. Measurement of strontium recoveries through both the in-growth of ^{90}Y and the use of ^{85}Sr as a tracer for gamma spectroscopy showed recoveries of greater than 80% using 2 mL pre-packed SR resin cartridges. During the in-growth method, ^{90}Sr was separated and each fraction collected from the separation was counted using the Liquid Scintillation Counter immediately after the separation and several times, days or even weeks after. Using set window

regions allowed for recovery yield analysis without the difficulty associated with broad peaks and peak shifting often associated with pure beta emitters. This technique worked, but was very time consuming, since the equilibrium of ^{90}Sr and ^{90}Y takes about ten days to reach. Therefore it is not useful in emergency response when measurements need to be known as soon as possible and immediate quantitative measurements of ^{90}Sr often require intensive calculations [25]. Using a tracer such as ^{85}Sr appeared to also work in determining the recovery yields of radiostrontium and with opportunity for shorter count times. This method cannot be used to determine the actual concentration of ^{90}Sr since the contribution of ^{90}Y was not accounted for. Depending on the activity of ^{85}Sr in the sample and/or the availability of an automated gamma spectrometer, each sample can take anywhere from several minutes to one day to count. In these studies, samples were counted for three hours in order to ensure adequate counting error for all samples. Inductively Coupled Plasma – Atomic Emission Spectroscopy was used for most samples as a third detection method to analyze where the stable, elemental, calcium and strontium eluted. The separations of radiostrontium in the presence of 0.1, 0.4, 0.6, and 0.8 M [Ca^{2+}] certified NIST samples and a 0.8 M [Ca^{2+}] generic Ebonex sample were compared. For all samples, except for roughly a 5% yield reduction for 0.1 M [Ca^{2+}], virtually all of the strontium was recovered.

Table 5 Combined average recoveries of strontium for all sets of data

BONE MATRIX	ICP-AES		LSC		GAMMA	
NIST-1400 [0.1M]	100.00%	± *3%*	98.00[1]%	± *5.1%*	95.00%	± *4.8%*
NIST-1400 [0.4M]	100.00%	± *0.4%*	99.61%	± *2.5%*	99.80%	± *2.4%*
NIST-1400 [0.6M]			92.80%	± *6.3%*	99.10%	± *11.5%*
NIST-1400 [0.8M]			91.30%	± *6.2%*	100.50%	± *5%*
NIST-1400 [3.3g]					78.80%	± *7.9%*
NIST-4356 [3.3g]					90.70%	± *10.9%*
EBONEX [0.1M]			100.20%	± *3.4%*		
EBONEX [0.8M]	97.80%	± *5%*	97.60%	± *3.1%*	100.70%	± *2.3%*
EBONEX [3.3g]					82.90%	± *5.4%*
LK MEAD [3.3g]					104.10%	± *6.7%*
IAEA [3.3g]					91.80%	± *7.6%*

[1] In-growth of yttrium-90 after a period of 7 days

For the separation run comparing 0.1 M and 0.4 M [Ca^{2+}] NIST and 0.8 M [Ca^{2+}] Ebonex, majority of elemental calcium present was eluted within the first two fractions; load and rinse. Elemental strontium was almost entirely removed in the strip fraction for all samples, except a small breakthrough of mostly stable, elemental strontium was observed for 0.8 M [Ca^{2+}] Ebonex containing samples.

A blank, certified IAEA-12 (0.38% magnesium and a 1.76 Ca:P ratio), generic Ebonex (0.83% magnesium, 8.62% aluminum, 1.76% potassium and a 1.64 Ca:P ratio), and two certified NIST samples (1.06% aluminum and a 1.60 Ca:P ratio and 0.89% magnesium with a 2.36 Ca:P ratio) were made up using 3.3 grams of the respective bone ash microwave digested in nitric acid for a final volume of 25 mL of 4 M nitric acid. The five samples matrices were added to the columns during the separation of radiostrontium and then analyzed. The separation analyzing the IAEA-12 yielded the highest recovery, of about 99% and the certified NIST-1400 sample without a radioactive spike yielded the lowest recovery at about 70%, possibly due to large amounts of calcium, phosphate, or due to the small amounts of magnesium present. Standard reference materials IAEA-12 and NIST 4356 as well as a bighorn sheep sample from Lake Mead, Nevada were prepared the same way as the previous samples, by mass comparison, and counted with Liquid Scintillation detection. Liquid scintillation data collected directly after separation revealed the highest number of counts from the Lake Mead sample giving rise to the slightly greater radiostrontium recovery of about 4% compared to the NIST and IAEA standards. Recoveries from the separation reached a high of 104%, this being most likely due to small geometric differences in counting of volumes close to the detector; the inverse square law. The results from gamma spectroscopy revealed a similar trend of increasing affinity for ^{85}Sr on the resin, the IAEA-12 standard had the lowest recovery at around 99%, NIST-4356 recovered around 103%, and the Lake Mead environmental sample recovered about 104% radiostrontium.

CHAPTER 5

5 CALCULATIONS & ERROR ANALYSIS

5.1 Data Analysis

5.1.1 Mean Calculations

The mean was calculated for all sets of data and further used to include the determination of the standard deviation. The equation for the mean, $\bar{x}$, is shown in Equation 5 below [22].

$$\bar{x} = \Sigma \frac{x_i}{N} \tag{5}$$

In this equation x_i represents the number of counts obtained for each sample under identical conditions and N is the number of samples.

5.1.2 Standard Deviation Calculations

The standard deviation, σ, of each individual sample was determined by Equation 6, shown below [22].

$$\sigma = \sqrt{x} \tag{6}$$

In this equation, x represents the number of counts of each sample. For a spectrum with a peak area of 10,000 counts, the relative error associated with the standard deviation would be 1 %, which is considered a very low error. The three hour count time used for gamma measurements resulted in roughly 20,000 counts for radiostrontium in samples counted early on in the studies, and no less than 1,000 counts for samples counted towards the end of the studies.

Using the mean, the deviation from the mean, or the standard deviation, for a set of samples was calculated for every set of samples measured. Microsoft Excel was used to calculate the mean and standard deviation calculations and the unbiased, or "n-1" method was used for these calculations. In this equation, x is the mean, x_i represents each sample value, and N is the number of samples. The standard deviation was calculated using Equation 7 below [22].

$$\sigma = \sqrt{\frac{\Sigma(\bar{x} - x_i)^2}{N-1}} \tag{7}$$

When combining individual samples, the standard deviation for the average of a collection of data points and/or for the count rate Equation 8 can be used [22].

$$\sigma_u = \sqrt{\sigma_x^2 + \sigma_y^2} \tag{8}$$

In this equation, σ_x and σ_y are the standard deviations of all samples involved.

5.1.3 Decay Correction Calculations

The radiostrontium standards used in the batch distribution and column separation studies decayed over time; therefore decay corrections were necessary, particularly for ^{85}Sr due to its 64.8-day half-life. For samples that contained these standards Equation 9 was used [22].

$$A_t = A_0 \cdot e^{-\lambda t} \tag{9}$$

In this equation A_t, the decay corrected activity, was determined by use of a known original activity, A_0, the decay constant (λ), or 0.693 / half-life (t ½), and the amount of time elapsed (t). Due to the three hour count time required and the absence of an automated gamma spectrometer, many samples in the batch distribution studies were counted after several half-lives of the ^{85}Sr had decayed, leaving sample activity relatively low. For this reason the activity counted in each sample was decay corrected back to the original activity representative of the beginning of the experiment. By manipulating Equation 10, the original activity, A_0, was calculated and is shown below as Equation 10 [22].

$$A_0 = \frac{A_t}{e^{-\lambda t}} \tag{10}$$

After a volume correction, using a ratio of the sample volume and the volume of solution interacted, these new activities were used for the calculations of the resin capacity factors values, k' trends.

5.1.4 Recovery Yield Calculations

At least 3 replicates, and up to five, were observed for each concentration or species of interest. The recovery of radiostrontium from the column studies and the batch studies required a comparison to the standard solutions using Equation 11 shown below:

$$\text{Recovery } (\%) = \frac{A_{X_i}}{A_y} \cdot 100 \tag{11}$$

In this equation Ax_i represents the activity of each sample in cpm (counts per minute) and A_y is the activity in cpm from the standard. For each individual sample, the background was subtracted prior to any calculations and the activities were decay corrected prior to calculating the percent recovery of radiostrontium using Microsoft Excel.

Additional error in the recovery of radiostrontium occurred due to error in the pipetting of solutions into the reservoir for column separation studies, mixing materials in the batch experiments, and general preparation of samples.

5.2 Gamma Spectroscopy Measurements

Most samples from the column separations studies and all samples from the batch distribution studies were counted on the gamma spectrometer. The number of counts and live measurement time were recorded for each sample. A background sample was observed as well as a representative standard prior to counting any samples. After background subtraction from each sample, the percent recoveries of radiostrontium using the following method were explored.

For samples in the batch experiments, particularly for the magnesium bromide concentrations, the weighted averages, x_{wav}, were calculated using Equations 12 and 13 below as a verification of the data set [23].

$$x_{wav} = \frac{\Sigma w_i x_i}{\Sigma w_i} \tag{12}$$

$$w_i = \frac{1}{\sigma_i^2} \tag{13}$$

In these equations, x_i represents analyte in the sample, w_i represents the statistical weight of the sample, and σ_i is the standard deviation.

5.2.1 Error during the Counting Process

Several causes for error were introduced into the pool of samples. Distance from the detector plays a huge role in the error of counts collected, since more emissions can be collected when more of the sample's surface is subtended. The geometry of the samples accounted for some of the error, as the positioning of the samples did not allow for a complete collection of the radiation emitted. The last few remaining samples had endured the most radioactive decay and were counted using the new well detector, which allowed for better counting statistics due to the deeper void of the sample holder and closer distance to the detector, covering more of the sample, and comparable recoveries to earlier counted samples were observed. The software Genie 2000 provided an error; however, errors for the samples in these studies were calculated using Equation 6 and 7 and recovery yields were calculated using Equation 11.

5.3 Liquid Scintillation Measurements

The number of counts with error, live measurement time, and tSIE quench factors were recorded for each sample. The count rate was reported in cpm (counts per minute) by the Tri-Carb liquid scintillation software. The 60-minute count time for each sample was enough to allow for less than 1% standard deviation for samples which contained ^{90}Sr and a 2% sigma was set. Higher yield samples contained more than 25,000 counts for a standard deviation error close to 1%. The software produced an error for each sample, however the standard deviation error was calculated for each sample and set of samples using Equations 6 and 7 and the recovery yields were calculated using Equation 11.

5.4 Inductively Coupled Plasma – Atomic Emission Spectroscopy Measurements

Standards were prepared and counted prior to all sets of samples analyzed. Calibration curves were created for each radiostrontium standard in order to insure the stability and precise behavior of the sample dilutions; R^2 values were greater than 0.999. The raw counts were collected and used to determine the yield of each element of interest as well as the errors associated with the counts. The equations for fitted lines from the standard calibration curves of intensity, counts per second, verses calculated concentration, ppm (parts per million), were used to extrapolate the actual concentration of the solutions for each set of sample intensities. Using Equation 14 below the concentration of each sample was determined in ppm.

$$Concentration(ppm) = \frac{\left(Intensity_{sample} - b\right)}{mx} \tag{14}$$

In this equation, the intensity values are in counts per second, b represents the y-intercept of a fitted line, and mx represent the slope and coefficient factor of a fitted line. The final concentrations were converted to moles per liters, or M, by using the molecular mass of each element. Standard deviations were calculated for each set of samples using Equation 7.

5.4.1 Error during the Sample Preparation Process

Often concentrations of samples were too high for the ICP-AES and therefore multiple dilutions were necessary for analysis of the samples. For this reason error was introduced into the samples through pipetting, but some of the error can be considered minimal due to the consistency in preparation for all samples. Also three samples were analyzed from each standard and sample while using the same source due to the way the instrument was programmed. This setup allows for more precise results, however, some accuracy was lost as a compromise.

CHAPTER 6

6 CONCLUSION

6.1 Overview

Two types of experiments, batch and column studies, were performed in order to determine elemental contributions on the separation of radiostrontium using SR resin purchased from Eichrom technologies. Prior to performance of the two studies, composition of bone ash samples was verified using X-ray Diffraction, XRD, and characterized with a Scanning Electron Microscope, SEM, supplied with a backscattered electron (BE) detector. From the SEM results, the contaminants within the sample were determined and quantified. Bone samples used in the following studies included a generic ashed matrix purchased from Ebonex Corporation, an environmental Nevada Bighorn Sheep sample that was pulverized in the laboratory, NIST-1400 and NIST-4356 standard reference materials, as well as an IAEA-12 certified reference standard.

6.2 Batch Experiments

Batch distribution studies were performed with the focus on adsorption effects from individual elements that are typically found in bone. The studies used 1.5 mL conical microcentrifuge vials, 0.5 mg of SR resin, and utilized a total volume of 1.3 mL, which consisted of prepared elemental solutions and an ^{85}Sr standard. The elemental solutions were prepared from aluminum chloride, calcium bromide, magnesium bromide, potassium bromide, potassium phosphate, and zirconium (IV) sulfate and diluted in 4 M nitric acid. An aliquot of the final filtered solution was assayed using Gamma Spectroscopy and the activity was used to determine the k' values, or resin capacity factors. The k' trends for the sorption of radiostrontium in the presence of the following elements were observed: potassium (I), calcium (II), magnesium (II), aluminum (III), zirconium (IV), and phosphate.

Shown in the trends of the k' values, calcium, potassium, phosphate, aluminum, and aluminum all played a role towards the sorption of radiostrontium onto the SR resin. Calcium greatly inhibited the retention of radiostrontium starting at concentrations somewhere between 0.1 M and 0.5 M calcium[2^+] and potassium greatly reduced the affinity for ^{85}Sr on the resin until a point of virtually no attraction to the resin was observed at about 0.5 M potassium [1^+]. Potassium, when in the presence of phosphate, seemed to also reduce the retention of radiostrontium to the resin, but not as significantly as in the absence of phosphate. Aluminum was shown to have a synergistic effect on the sorption of radiostrontium beginning at a concentration of 0.26 M aluminum [3^+]. Magnesium had a peculiar trend that reduced the affinity of radiostrontium to the SR resin up until 0.59 M magnesium [2^+], at which point the sorption of ^{85}Sr to the resin is preferred and is enhanced to a point of synergism at roughly 5.3 M magnesium [2^+]. Zirconium did not play a role in the sorption of radiostrontium in this study.

6.3 Column Studies

The column separation studies followed and the investigation was geared towards the overall effect of various bone matrices on the separation of radiostrontium. Bone ash samples were prepared using a microwave digestion system and diluted in nitric acid. The solutions, with a known aliquot of either ^{90}Sr or with the addition of tracer ^{85}Sr, were then added to the columns and allowed to interact with SR resin cartridges purchased from Eichrom technologies. The separation was divided up into four fractions: wet, load, rinse, and strip, and carried out using a vacuum assisted pressurized box at a fixed setting of 675 torr. The load, rinse, and strip phases were counted using Liquid Scintillation detection, and/or Gamma Spectroscopy and Inductively Coupled Plasma – Atomic Emission Spectroscopy. The recovery rates were determined for the various sample matrices by comparing the count rates from LS detection and Gamma Spectroscopy to a radiostrontium standard. The ICP-AES data was used to observe the elemental

behaviors of elemental calcium and strontium in the fractions during the separation due to the complexity of the in-growth of ^{90}Y.

Original recovery values of ^{90}Sr by LS detection were low, between 40 and 60 %, and large amounts of breakthrough in the load and rinse phase were observed. The contribution from the in-growth of daughter product ^{90}Y let to this anomaly and an in-growth experiment was performed as well as a tracer experiment using gamma detection of isotope ^{85}Sr. The in-growth method observed the recovery rates of radiostrontium immediately after separation, day 42, and day 77 (previously shown in Figure 27). This study verified the contribution from yttrium to the load, rinse, and strip fractions and the recovery values improved to greater than 80% for radiostrontium. Several samples ran also include a tracer isotope of ^{85}Sr, which was collected and gamma detection revealed greater than 90% recovery for most samples (see Table 5). ICP-AES was also used to verify in which of the separation fractions contained strontium. The results, shown in Table 5, indicate that greater than 98% of the strontium present in the sample is primarily in the strip fraction.

6.4 Future Work

Continuation of this work should include the investigation of dissolution techniques for other urban rubble materials such as rebar, cement, asphalt, molten glass, and steel. The morphology and composition of the samples could be observed using SEM and XRD as a minimum prior to dissolution and then followed by separation using extraction chromatography if dissolution is successful. The elements of interest can be expanded to include alpha emitting isotopes and specific isotopic ratios can be observed. Batch experiments can be carried out for elements that may be present in the materials not previously found in bone ash. Finally crystals of the elements of interest with the ligands utilized on the Eichrom resins can be grown and observed by SEM and XRD in order to better understand the chemical interactions associated with the extraction process.

APPENDIX I

CHEMICALS

Nitric acid, ACS Grade

CAS 7697-37-2

Aluminum chloride, anhydrous, 99.985% (metals basis), Alfa Aesar

CAS 7446-70-0

Aluminum nitrate, Sigma Aldrich

CAS 7784-27-2

Calcium bromide, anhydrous, 99.5%, Alfa Aesar

CAS 7789-41-5

Calcium hydroxide, powder, BAKER ANALYZED ACS Reagent, J.T. Baker

CAS 1305-62-0

Magnesium bromide hexahydrate, Acros Organics

CAS 13446-53-2

Potassium phosphate, monobasic, Laboratory Grade, Fisher Scientific

CAS 7778-77-0

Potassium bromide, ReagentPlus, ≥ 99.0%, Sigma-Aldrich

CAS 7758-02-3

Zirconium (IV) Sulfate, tetrahydrate, 98+%, Alfa Aesar

CAS 7446-31-3

^{90}Sr, Isotope Products

^{85}Sr, Isotope Products

APPENDIX II

MATERIALS AND REAGENTS

^{90}Sr in 4 mol L^{-1} nitric acid, 100 Bq mL^{-1}

^{90}Sr in 4 mol L^{-1} nitric acid, 200 Bq mL^{-1}

^{85}Sr in 4 mol L^{-1} nitric acid, 500 Bq mL^{-1}

^{85}Sr in 4 mol L^{-1} nitric acid, x Bq mL^{-1}, Isotope Products

^{85}Sr in 4 mol L^{-1} nitric acid, x Bq mL^{-1}, Isotope Products

SR resin cartridges, Eichrom Technologies

SR resin, loose, Eichrom Technologies

Bone ash, 325 Mesh, Ebonex Co.

Bone ash, Standard Reference Material 1400, NIST

Bone ash, Standard Reference Material 4356, NIST

Bone ash, Standard Reference Material 12, IAEA

Bone, Bighorn Sheep, Lake Mead Nevada

Nitric acid, 4 mol L^{-1}

Nitric acid, 5 mol L^{-1}

Nitric acid, 8 mol L^{-1}

Aluminum nitrate, 0.5 mol L^{-1}

Planetary Ball Mill PM 100, Retsch

Mortar and Pestle

Thermo Scientific Labquake Shaker (fixed speed)

Whatman PTFE membrane Syringe Filters, 0.45 µm pore size

APPENDIX III

Table 6 Data presented in Figure 19.
Average k' values for mixing times of 1 hour, 6 hours, and 24 hours of 50 mg of SR resin

Mixing Time	**k' values**	
1 Hour		
	14.11	± *0.007*
	14.91	± *0.008*
	14.94	± *0.008*
	15.34	± *0.008*
	15.14	± *0.008*
6 Hours		
	15.05	± *0.008*
	15.36	± *0.008*
	15.74	± *0.009*
	15.88	± *0.009*
24 Hours		
	15.52	± *0.008*
	14.70	± *0.008*
	14.36	± *0.009*
	15.46	± *0.009*
	15.50	± *0.010*

Table 7 Data presented in Figures 20 – 25
Contributions from ionic solutions on the separation of radiostrontium.

Ionic Species	**Concentration [M]**	**k' values**	
Calcium [2^+]			
	0.0	14.65	± *0.052*
	0.1	12.70	± *0.496*
	0.2	1.17	± *0.429*
	0.3	0.90	± *0.193*
	0.4	0.90	± *0.202*
	0.5	0.82	± *0.168*
	1.0	1.09	± *0.237*
	2.5	2.29	± *0.147*

Ionic Species	Concentration [M]	k' values	
Potassium [1^+] in the presence of phosphate			
	0.0	15.04	± *0.472*
	0.1	8.31	± *0.525*
	0.3	5.12	± *0.376*
	0.5	3.70	± *0.219*
	0.7	2.91	± *0.279*
	1.0	1.82	± *0.220*
Ionic Species	**Concentration [M]**	**k' values**	
	2.0	1.05	± *0.306*
	3.0	0.79	± *0.139*
	3.5	0.67	± *0.152*
Potassium [1^+] in the absence of phosphate			
	0.0	62.85	± *2.253*
	0.1	37.36	± *1.727*
	0.2	25.15	± *0.794*
	0.3	5.43	± *0.624*
	0.4	1.81	± *0.358*
	0.5	0.71	± *0.379*
	1.0	-0.50	± *0.462*
	2.0	-0.20	± *0.389*
	3.0	0.02	± *0.298*
	4.0	0.12	± *0.189*
	5.3	0.08	± *0.185*
Magnesium [2^+]			
	0.0	62.85	± *2.253*
	0.1	53.83	± *3.017*
	0.3	0.75	± *0.156*
	0.5	0.58	± *0.064*
	1.0	2.72	± *0.040*
	4.0	66.39	± *3.211*
Aluminum [3^+]			
	0.0	59.11	± *2.683*
	0.1	57.24	± *2.246*
	0.3	64.53	± *2.653*
	0.5	63.62	± *1.249*
	1.0	76.38	± *2.967*
	1.5	82.45	± *8.093*
	3.0	96.59	± *5.355*
Zirconium [4^+]			
	0.0	0.38	± *0.396*
	0.1	59.31	± *2.199*
	0.3	59.49	± *2.785*
	0.5	61.73	± *3.118*
	1.0	62.05	± *3.092*

Table 8 Data presented in Figure 26
Recovery of radiostrontium at various pressure settings

	Radiostrontium Recovery		
650 Torr			
	0.25	± 0.049	*Load*
	0.05	± 0.025	*Rinse*
	0.65	± 0.079	*Strip*
675 Torr			
	0.06	± 0.027	*Load*
	0.01	± 0.016	*Rinse*
	0.88	± 0.091	*Strip*
690 Torr			
	0.30	± 0.054	*Load*
	0.07	± 0.029	*Rinse*
	0.60	± 0.075	*Strip*

Table 9 Data presented in Figure 27
Recovery of radiostrontium in the presence of 0.1 M Ebonex bone ash using the in-growth of ^{90}Y

	Radiostrontium Recovery		
0 Days			
	0.11	± 0.128	*Load*
	0.08	± 0.099	*Rinse*
	0.61	± 0.144	*Strip*
42 Days			
	-0.01	± 0.082	*Load*
	-0.01	± 0.082	*Rinse*
	0.94	± 0.161	*Strip*
77 Days			
	0.00	± 0.053	*Load*
	0.00	± 0.077	*Rinse*
	0.98	± 0.159	*Strip*

Table 10 Data presented in Figure 28

Total recovery of elemental calcium for selected bone ash matrices	Elemental Calcium Recovery		
0.1 M NIST			
	0.80	± 0.007	*Load*
	0.19	± 0.005	*Rinse*
	0.01	± 0.009	*Strip*
0.4 M NIST			
	0.68	± 0.001	*Load*
	0.32	± 0.008	*Rinse*
	0.00	± 0.009	*Strip*
0.8 M EBONEX			
	0.65	± 0.100	*Load*
	0.34	± 0.008	*Rinse*
	0.00	± 0.025	*Strip*

Table 11 Data presented in Figure 30
Recovery of radiostrontium in the presence of various concentrations of bone ash

Sample Matrix	Radiostrontium Recovery	
0.1 M NIST	0.95	± *0.046*
0.4 M NIST	1.00	± *0.045*
0.6 M NIST	1.00	± *0.056*
0.8 M NIST	1.02	± *0.056*
0.8 M EBONEX	1.01	± *0.055*

Table 12 Data presented in Figure 31
Recovery of radiostrontium in the presence of various bone ash matrices made up of 3.3 g bone ash and dissolved to a total volume of 25 mL and a concentration of 4 M nitric acid

Sample Matrix	Radiostrontium Recovery	
Blank	0.89	± *0.043*
IAEA12	0.90	± *0.042*
NIST 4356	0.83	± *0.043*
EBONEX 325	0.76	± *0.044*
NIST 1400	0.69	± *0.045*

Table 13 Data presented in Figure 32
Recovery of radiostrontium in the presence of various bone ash matrices made up of 3.3 g bone ash and dissolved to a total volume of 25 mL and a concentration of 4 M nitric

	Radiostrontium Recovery		
IAEA 12			
	0.58	± 0.003	*Load*
	0.59	± 0.003	*Rinse*
	0.58	± 0.003	*Strip*
NIST 4356			
	0.59	± 0.003	*Load*
	0.58	± 0.003	*Rinse*
	0.60	± 0.003	*Strip*
LAKE MEAD			
	0.61	± 0.003	*Load*
	0.61	± 0.003	*Rinse*
	0.61	± 0.003	*Strip*

Table 14 Data presented in Figure 33
Recovery of radiostrontium in the presence of various bone ash matrices made up of 3.3 g bone ash and dissolved to a total volume of 25 mL and a concentration of 4 M nitric acid

Sample Matrix	Radiostrontium Recovery	
IAEA 12	1.00	± 0.027
NIST 4356	1.03	± 0.027
LAKE MEAD	1.04	± 0.027

BIBLIOGRAPHY

1. Tovedal, A.; Nygren, U.; Ramebäck, H. Determination of ^{90}Sr in preparedness: Optimization of total analysis time for multiple samples. *J. Radioanal. Nucl. Chem.* **2008**, 276, 357-362.
2. *Background material for the development of radiation protection standards protective action guides for strontium-89, strontium-90 and cesium-137*. Report No. 7; Staff Report of the Federal Radiation Council, U.S. Government Printing Office: Washington, D.C., May 1965.
3. Vajda, N; Kim, C; Determination of radiostrontium isotopes: A review of analytical methodology. *Journal of Applied Radiation and Isotopes*, **2010**, *68*, 2306 – 2326.
4. Papworth, D.; Vennart, J.; The uptake and turnover of ^{90}Sr in the human skeleton. Phys. Med. Biol., **1984**, *29*: 1045.
5. Alpen, Edward L. Radiation Biophysics, 2nd ed.; Academic Press, 1998.
6. Chmielewska, I.; Chalupnik, S.; Bokori, E. *Application of Calcium Carrier to Avoid Losses of ^{90}Sr During the Chemical Preparation of Liquid Samples for Liquid Scintillation Spectrometry*. LSC International Conference. Davos, Switzerland. 2008.
7. Tovedal, A.; Nygren, U.; Lagerkvist, P.; Versterlund, A.; Ramebäck, H. Methodology for determination of ^{89}Sr and ^{90}Sr in radiological emergency: II. Method development and evaluation. J. Radioan. Nucl. Chem. 2009, 282, 461 – 466.
8. "Extraction Chromatography of actinides and Selected Fission Products: Principles and Achievement of Selectivity." Eichrom Technologies, Inc. 2007 <www.eichrom.com>.
9. Horwitz, P.; Chiarizia, R.; Dietz, M. *A Novel Strontium Selective Extraction Chromatographic Resin*. Chemistry Division, Argonne National Laboratory. Argonne, IL. 1992.
10. Pilviö, R.; Bickel, M. Separation of actinides from a bone ash matrix with extraction chromatography. *J. Alloys Compd*. **1998**, 271 – 273, 49 – 53.
11. Horwitz, E.; McAlister, D; Extraction Chromatography Versus Solvent Extraction: How Similar Are They? *Journal of Separation Science and Technology*, **2006**, *41*, 2163-2182.

12. Maxwell, S. L.; Culligan, B. K. Rapid method for determination of radiostrontium in emergency milk samples. *J. of Radioan. Nucl. Chem*. **2009**, 279, 757 – 760.

13. Maxwell, S. L. Rapid column extraction method for actinides and $^{89/90}$Sr in water samples. *J. Radioan. Nucl. Chem.* **2006**, 267, 537 – 543.

14. Jäggi, M.; Eikenberg, J. Separation of ^{90}Sr from radioactive waste matrices – Microwave versus fusion decomposition. . *Int. J. Radiat. Applic. Instrum., Part A*. **2009**, 67, 765 - 769.

15. Kelly, L. R. Optimization of the microprecipitation procedure for nuclear forensics applications. M.S. Thesis, University of Nevada Las Vegas, 2009.

16. Sanchez, A. L.; Singleton, D. L. A Radioanalytical Scheme for Determining Transuranic Nuclides and ^{90}Sr in Environmental Samples. *J. Radioan. Nucl. Chem.* **1996**, 209, 41 – 50.

17. Stamoulis, K.C.; Assimakopoulos, P.A., Ioannides, K.G.; Jonson, E.; Soucacos, P.N. Strontium-90 concentration measurements in human bones and teeth in Greece. *Sci. Total. Environ.* **1999**, 229, 165 – 182.

18. Filipy, R; Alldredge, J; Hall, C; McInroy, J; Glover, S; Qualls, S; Estimation of Actinide Sketal Content Based on Bone Samples Collected at Autopsy. United States Transuranium and Uranium Registries, Washington State University, Tri-cities. Health Physics Society. 2002.

19. EPA Method, "Milestone." Milestone Microwave Laboratory Systems, Web. 4 May 2009. <http://www.milestonesci.com/dig-resources.php>.

20. University of Wisconsin – Milwaukee Environmental Health, Safety, and Risk Management Radiation Safety Program. www.ehs.psu.edu/radprot/**LSC**_Theory1.pdf. (accessed October 15, 2010).

21. Krane, K.*; Introductory Nuclear Physics*; John Wiley & Sons Inc, 1987; pp 202.

22. Knoll, G.; *Radiation Detection and Measurement,* 3rd ed, John Wiley & Sons Inc., 2010.

23. Taylor, J.; *An Introduction to Error Analysis: The Study of Uncertainties in Physical Measurements*, 2nd ed.; Sausalito, CA, 1982; 173 – 179.

24. Heckel, A.; Vogl, K. Rapid method for determination of the activity concentrations of ^{89}Sr and ^{90}Sr. *Int. J. Radiat. Applic. Instrum., Part A*. **2009**, 67, 794 – 796.

25. Qu, H; Stuit, D; Glover, S; Love. S; Filby, R; Preconcentration of plutonium and americium using the Actinide –CUTM Resin for human tissue analysis, *Journal of Radioanalytical and Nuclear Chemistry*, **1998**, *234*, 175 – 181.

26. Pilviö, R.; LaRosa, J. J.; Mouchel, D.; Wordel, R.; Bickel, M.; Altitzoglou, T.; Measurement of low-level radioactivity in bone ash. *Journal of Environmental Radioactivity,* **1999**, *43,* 343-356.

27. Georgia State University Department of Physics and Astronomy. Hyperphysics. http://hyperphysics.phy-astr.gsu.edu/hbase/hframe.html (accessed November 7, 2011)

CURICULUM VITAE

Graduate College
University of Nevada, Las Vegas

Ashlee R. Dailey (Crable)

Degrees:

Bachelor of Arts, Chemistry, 2007
University of Nevada, Las Vegas

Bachelor of Arts, German, 2005
University of Nevada, Las Vegas

Thesis Title:

Elemental Contributions from Minor and Major Constituents of Bone on the Separation of Radiostrontium

Thesis Examination Committee:

Chairperson, Ralf Sudowe, Ph.D.
Co-Chairperson, Kenneth R. Czerwinski, Ph.D.
Committee Member, Kathleen A. Robins, Ph.D.
Committee Member, David W. Hatchett, Ph.D.
Committee Member, Kenton J. Moody, Ph.D.
Graduate Faculty Representative, Ralph Buechler, Ph.D.